ACS Chemical Neuroscience

Article

Design, synthesis, and biological evaluation of novel multifunctional Rolipram-Tranilast hybrids as potential treatment for traumatic brain injury

Junfeng Lu, Chen Chen, Xiaobing Deng, Marvin SH Mak, Zeyu Zhu, Xixin He, Jinhao Liang, Swetha K. Maddili, Karl W.K. Tsim, Yifan Han, and Rongbiao Pi

ACS Chem. Neurosci., **Just Accepted Manuscript** • DOI: 10.1021/acschemneuro.0c00339 • Publication Date (Web): 09 Jul 2020

is published by the American Chemical Society. 1155 Sixteenth Street N.W., Washington, DC 20036

Design, synthesis, and biological evaluation of novel multifunctional Rolipram-Tranilast hybrids as potential treatment for traumatic brain injury

Junfeng Lu[1§], Chen Chen[1§], Xiaobing Deng[2§], Marvin SH Mak[3,4], Zeyu Zhu[1], Xixin He[5], Jinhao Liang[5], Swetha K. Maddili[6], Karl W. K. Tism[4], Yifan Han[3], Rongbiao Pi [6,7,8*]

1. School of Pharmaceutical Sciences, Sun Yat-Sen University, Guangzhou 510006, China;

2. Peking-Tsinghua Center for Life Sciences, Peking University, Beijing 100871, China;

3. Department of Applied Biology and Chemical Technology, Institute of Modern Chinese Medicine, The Hong Kong Polytechnic University, Hung Hom, Hong Kong;

4. Division of Life Science and Center for Chinese Medicine, The Hong Kong University of Science and Technology, Hong Kong, China;

5. School of Pharmaceutical Sciences, Guangzhou University of Chinese Medicine, Guangzhou, China;

6. School of Medicine, Sun Yat-Sen University, Guangzhou 518000, China;

7. National and Local United Engineering Lab of Drugability and New Drugs Evaluation, Sun Yat-Sen University, Guangzhou 510006, China;

8. International Joint Laboratory<SYSU-PolyU HK> of Novel Anti-Dementia Drugs of Guangzhou, Guangzhou 510006, China.

[§] The first three authors contributed equally.

Abstract

Traumatic brain injury (TBI) is a prevalent public healthcare concern frequently instigated by mechanical shock, traffic or violence incidents, leading to permanent nerve damage and there is no ideal treatment for it yet. In this study, a series of Rolipram-Tranilast hybrids were designed and synthesized. The neuroprotective activities of the Rolipram-Tranilast hybrids were evaluated both in vitro and in vivo. Compound **5** has been identified as the strongest neuroprotective molecule among the series with robust anti-oxidant and anti-inflammatory potentials. Compound **5** significantly increased the heme oxygenase-1 (HO-1) levels and the phosphorylated cAMP response elements binding protein (p-CREB), while it down-regulated phosphodiesterase-4 B (PDE4B) expression in vitro. Furthermore, compound **5** remarkably attenuated TBI and had good safety profile in mice. Taken together, our findings suggested that compound **5** could serve as a novel promising lead compound in the treatment of TBI and other central nervous system (CNS) diseases associated with PDE4B and oxidative stress.

Keywords: Rolipram; Tranilast; CREB; inflammation; oxidative stress; neuroprotection; traumatic brain injury

Graphical abstract

Compound **5**, a Rolipram-Tranilast hybrid attenuated TBI by mutitargeted function in mice.

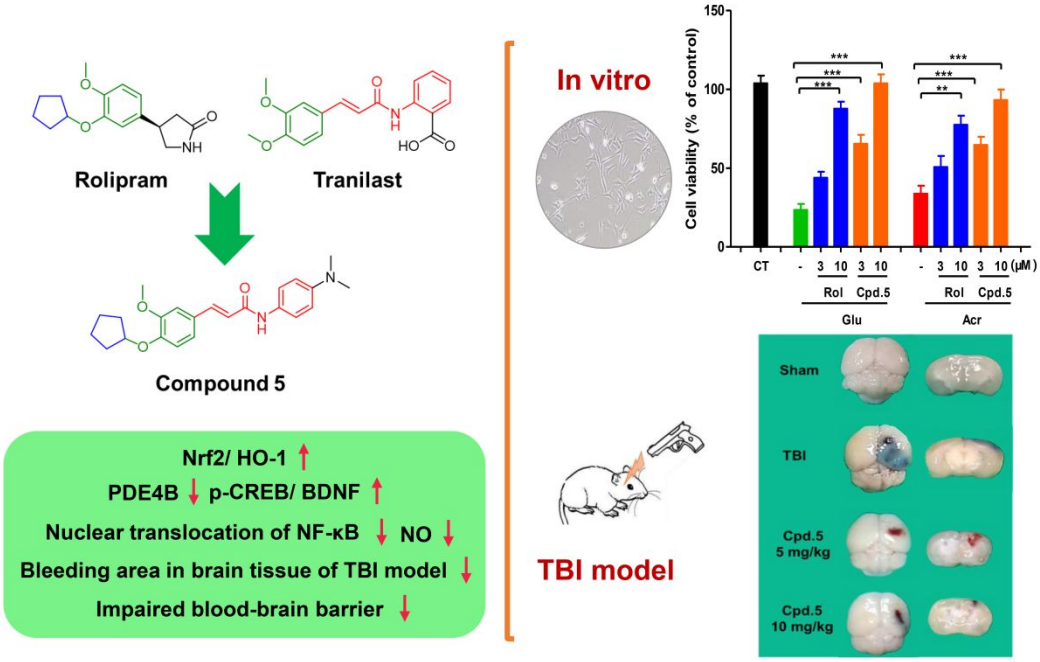

Introduction

Traumatic brain injury (TBI) is a prevalent public healthcare concern frequently caused by mechanical shock, traffic or violence incidents, leading to permanent nerve damage together with a wide range of symptoms and sequelae.[1] More than 50 million people are suffering from TBI annually worldwide.[2] TBI has become one of the foremost causes of death among the under 40 year-age groups in the developed countries. The brain damage induced by TBI can be separated into two phases, including primary and secondary effects. The mechanisms underlying TBI are very complex and multiple factors are involved in such neuropathological processes. Excitotoxicity, neuroinflammation, cytokine damage, oxidative stress injury, and eventual cell death are prominent mechanisms of neuronal loss

in the post TBI.[3,4,5] Currently, there is still no precise and ideal therapeutic strategy for the prevention of pathogenesis and neurodegeneration following TBI. Many potential candidates could not pass the clinical trials to date, and the "magic bullet" for effectively treating TBI-induced damage does not exist.[6,7] Given that the pathophysiological processes of primary and secondary injury of TBI are complex, "one-target" drug could not offer ideal therapeutic efficiency against TBI. Hence, multi-targeted drugs should be promising candidates for the treatment of TBI.[8,9] Moreover, it was found that in hippocampus, phosphodiesterase (PDE) expression has been increased during TBI, and inhibition of PDE might reverse the chronic cognitive deficits induced by TBI, suggesting that PDE should be a promising drug target against TBI.[10,11]

Rolipram, a pan-phosphodiesterase-4 (PDE4) inhibitor with significant neuroprotective effect, has been initially developed as a potential antidepressant.[12,13] It can penetrate the blood-brain barrier (BBB) and accumulate in the brain. In recent years, several studies have demonstrated that Rolipram exhibited therapeutic benefits in the neurodegenerative diseases (NDDs), such as TBI and Alzheimer's Disease.[14,15] In addition, Rolipram might also significantly improve hippocampal long-term potentiation (LTP) and learning after TBI.[16] Indeed Rolipram has passed in phase II clinical trials for multiple sclerosis and phase I for Huntington's Disease.[17,18] It should be highlighted that Rolipram has some intolerable adverse effects, such as nausea and vomiting, which may blocked its way to be used clinically.[15] Several laboratories have tried to develop derivatives of Rolipram by modifying the chemical structure.[19,20]

Tranilast (N-[3′,4′-dimethoxycinnamoyl]-anthranilic acid), an analogue of a tryptophan metabolite, is an anti-allergic agent which might be used in the treatment of inflammatory diseases.[21-23] Recently, studies have showed that Tranilast is a potential drug to alleviate life-threatening inflammatory response.[24] Additionally, Tranilast could attenuate cerebral ischemia-reperfusion injury by regulating the inflammatory cytokine production and PPAR expression.[21] These results suggest that Tranilast might be a good anti-inflammatory drug for many diseases, including NNDs. Although the detail mechanisms are not fully revealed, several studies reported that Tranilast could increase heme oxygenase-1 and exert potent anti-inflammatory effects.[25,26] Moreover, Tranilast was also found to decrease the production of reactive oxygen species (ROS).[27] These characters of Tranilast might be to the benefit of TBI. Unfortunately, Tranilast couldn't be used for the treatment of TBI, because of poor ability to penetrate the blood-brain barrier (BBB). It has been reported that the ratio of concentrations in plasma to brain is over 100 after an oral administration of Tranilast (10.5 mg kg^{-1}) in rats.[28]

Given that TBI is a complex pathological disease, multitarget compounds should be a powerful tool for the treatment of TBI.[8,29] We hypothesized that combinational effects of Rolipram and Tranilast should contribute to combating TBI. Here a series of Rolipram-Tranilast hybrids have been designed and synthesized by combining the 3-(cyclopentyloxy)-4-methoxybenzene moiety of Rolipram with the N-phenylcinnamamide nucleus of Tranilast (Figure 1 and Scheme 1). After evaluation, compound **5** was demonstrated to be the multifunctional lead compound for the treatment of TBI or other NNDs associated with PDE4B and oxidative stress.

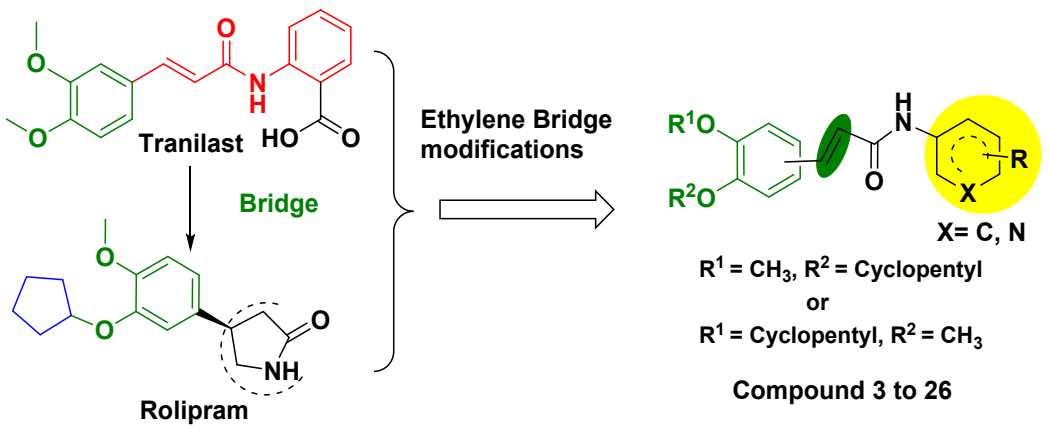

Figure 1. Design of novel Rolipram-Tranilast hybrids.

Results and Discussion.

Chemistry

General synthetic procedure for compounds **3-26** is depicted in Scheme 1. The appropriate acrylic acid (**1a** or **1b**) was treated with concentrated sulfuric acid in anhydrous ethanol at reflux to yield the ethyl ester **2a** or **2b**, which was then reacted with bromocyclopentane to yield product 3a or 3b. Next, the hydrolysis of **3a, b** in 20% sodium hydroxide and tetrahydrofuran afforded the final intermediate 3-(4-(cyclopentyloxy)-3-methoxyphenyl) acrylic acid (**4a**) or 3-(3-(cyclopentyloxy)-4-methoxyphenyl) acrylic acid (**4b**). Subsequently, analogues **3-26** were easily accessible by condensation reaction of carboxylic acid with different substituted amines using HBTA and EDCI as condensing agents in anhydrous dichloromethane at room temperature.

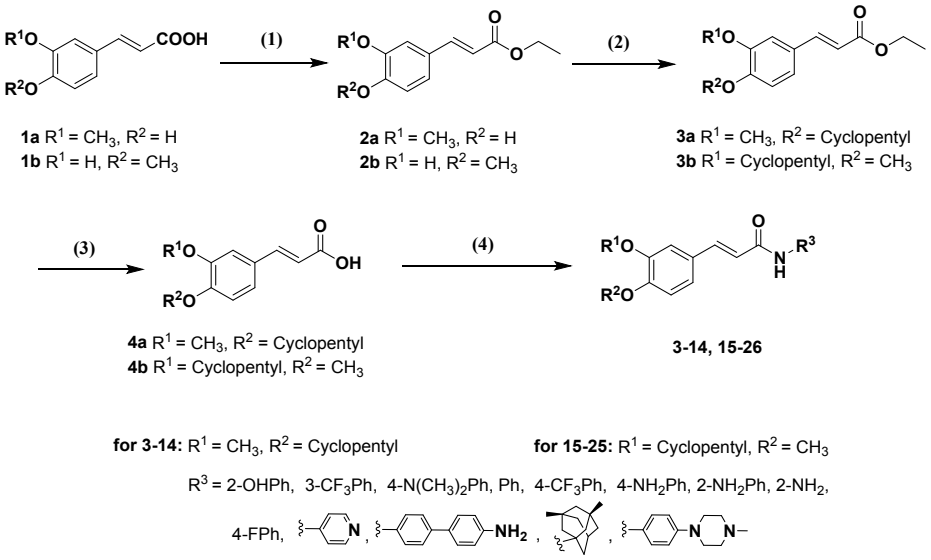

Reagents and conditions: (1) H_2SO_4 conc., ethanol, reflux; (2) Bromocyclopentane, K_2CO_3, DMF,65^oC; (3) 20% NaOH, THF, reflux; (4) RNH_2,EDCI, HOBt ,DCM, rt.

Scheme 1. Synthesis of the target compounds 3-26.

Pharmacology Evaluation In vitro

Table 1. Neuroprotective and cytotoxic effects of compounds in HT22 cells.

Compd.	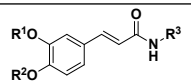			Cytotoxicity	Glutamate (3 mM)		Acrolein (20 μM)	
	R^1	R^2	R^3	100 μM	3 μM	10 μM	3 μM	10 μM
3	CH_3	C_5H_9	2-OHPh	54.1 ± 2.3	24.7 ± 0.8	46.0 ± 1.8	45.5 ± 0.5	49.3 ± 1.2
4	CH_3	C_5H_9	3-CF_3Ph	33.1 ± 1.3	24.8 ± 0.9	42.3 ± 0.6	42.0 ± 1.2	52.4 ± 0.7
5	CH_3	C_5H_9	4-$N(CH_3)_2$Ph	103.4 ± 1.3	75.8 ± 1.3	100.5 ± 1.2	72.8 ± 1.2	96.4 ± 1.4
6	CH_3	C_5H_9	Ph	69.7 ± 2.5	24.6 ± 0.4	56.5 ± 1.5	39.4 ± 1.1	52.6 ± 0.5
7	CH_3	C_5H_9	4-CF_3Ph	47.2 ± 1.8	28.0 ± 0.7	54.7 ± 0.6	37.7 ± 0.7	43.0 ± 0.6
8	CH_3	C_5H_9	4-NH_2Ph	83.5 ± 2.6	50.2 ± 1.4	81.3 ± 1.5	40.3 ± 0.6	79.2 ± 0.6
9	CH_3	C_5H_9	2-NH_2Ph	43.1 ± 1.3	27.7 ± 0.8	57.1 ± 1.5	38.9 ± 0.9	62.7 ± 1.2
10	CH_3	C_5H_9	2-NH_2,4-FPh	64.8 ± 1.9	24.0 ± 0.5	44.3 ± 1.4	37.1 ± 0.5	60.9 ± 1.0
11	CH_3	C_5H_9		23.7 ± 1.8	23.9 ± 0.9	51.7 ± 0.7	34.8 ± 0.7	43.6 ± 0.7
12	CH_3	C_5H_9	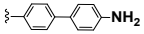	20.3 ± 1.8	25.0 ± 0.8	52.7 ± 0.7	36.0 ± 1.2	49.1 ± 1.4
13	CH_3	C_5H_9		84.4 ± 0.9	25.9 ± 1.7	46.5 ± 1.5	38.0 ± 1.0	43.8 ± 0.4
14	CH_3	C_5H_9	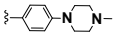	58.0 ± 1.0	52.2 ± 0.7	65.4 ± 1.3	42.7 ± 0.6	63.1 ± 0.5
15	C_5H_9	CH_3	2-OHPh	34.9 ± 1.0	27.1 ± 1.1	66.1 ± 1.7	40.6 ± 0.6	56.8 ± 0.6
16	C_5H_9	CH_3	3-CF_3Ph	32.6 ± 1.0	25.8 ± 0.9	44.8 ± 1.5	37.0 ± 0.6	61.6 ± 1.2

17	C_5H_9	CH_3	4-$N(CH_3)_2$Ph	81.6 ± 1.3	60.2 ± 1.6	81.0 ± 0.9	51.9 ± 0.6	72.8 ± 0.6
18	C_5H_9	CH_3	Ph	80.7 ± 0.8	26.4 ± 0.5	46.3 ± 1.9	37.4 ± 0.5	45.5 ± 0.5
19	C_5H_9	CH_3	4-CF_3Ph	70.0 ± 1.5	27.8 ± 0.9	56.3 ± 1.0	36.0 ± 0.4	50.2 ± 1.1
20	C_5H_9	CH_3	4-NH_2Ph	53.6 ± 2.0	54.4 ± 0.6	73.6 ± 1.3	56.1 ± 0.7	73.2 ± 1.0
21	C_5H_9	CH_3	2-NH_2Ph	66.3 ± 1.3	27.5 ± 0.7	44.1 ± 1.1	36.5 ± 0.4	63.4 ± 0.7
22	C_5H_9	CH_3	2-NH_2,4-FPh	64.6 ± 1.9	26.8 ± 0.7	67.2 ± 0.8	36.8 ± 0.5	74.0 ± 0.4
23	C_5H_9	CH_3		21.7 ± 2.3	29.3 ± 1.2	61.6 ± 0.7	36.7 ± 0.4	50.9 ± 1.0
24	C_5H_9	CH_3	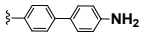	39.2 ± 1.1	30.5 ± 1.3	51.8 ± 0.9	36.1 ± 0.4	46.4 ± 0.3
25	C_5H_9	CH_3		67.9 ± 2.0	29.5 ± 0.8	42.0 ± 0.8	39.9 ± 0.6	44.7 ± 0.6
26	C_5H_9	CH_3	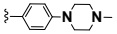	59.0 ± 1.7	43.3 ± 0.6	69.7 ± 1.0	40.4 ± 1.0	52.4 ± 0.7
		Rolipram		87.1 ± 1.2	39.8 ± 1.8	85.4 ± 1.8	54.6 ± 1.1	78.4 ± 0.9

Note: The table showed that the cytotoxicity of the compounds at 100 μM and neuroprotective effects against glutamate- and acrolein-induced neuronal injury at 3 and 10 μM in HT22 cells. The cell viability was expressed as the percentage of control group. The data were expressed as the mean ± SD, n = 6.

Compound 5 prevented the cell death against glutamate- or acrolein-induced damage in HT22 cells.

We speculated that the Rolipram-Tranilast hybrids might provide neuroprotection effects. HT22 cells, a mouse hippocampal cell line, were used to evaluate sequential oxidative stress and cell death cascade triggered by glutamate- or acrolein- induced cell injury. The activities of these compounds against cell injuries were shown in Table 1. On the basis of the results, compound **5** was selected as for further study. Using phase contrast microscopy, we found that compound **5** reversed cell death induced by glutamate or acrolein (Figure 2A) and no cytotoxicity was observed under 100 μM in HT22 cells. In addition, compound **5** significantly reduced the glutamate- or acrolein-induced cytotoxicity (Figure 2B, C).

Rolipram is a specific inhibitor of PDE4.[13] It was reported to benefit to NDDs, including brain trauma.[30] The nuclear factor-related factor 2 (Nrf2) pathway is the key regulatory hub of endogenous antioxidant system.[19] Under oxidative stress, Nrf2 is activated and initiates downstream gene transcription, and up-regulates the expression of endogenous antioxidant enzymes, such as heme oxygenase (HO), so as to improve the antioxidant capacity of cells.[31-33] HO-1, one of the major targeted genes of Nrf2, has potent antioxidant and anti-inflammatory effects and is found to have important roles in NDDs or ischemic and hypoxic coronary artery disease.[33,34] The neuroprotection of compound **5** was better than that of Rolipram (Figure 2C). Further study showed that compound **5** significantly upregulated the level of HO-1(Figure 2D).

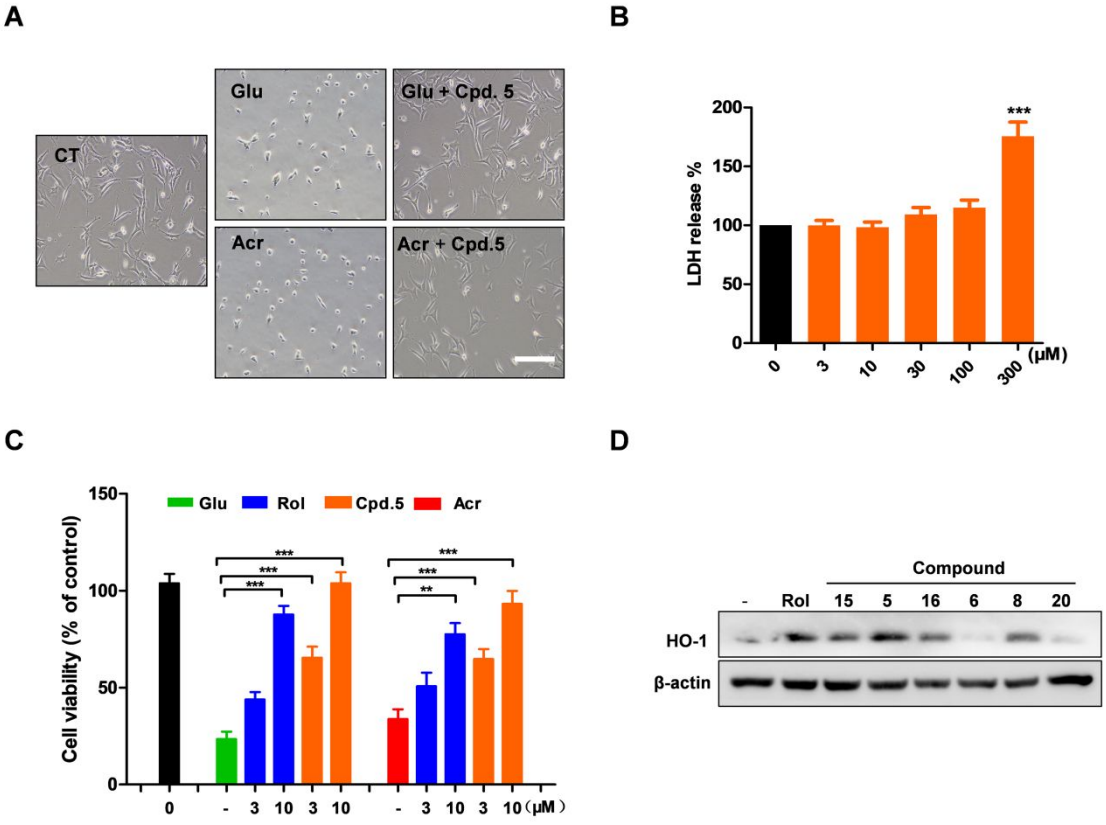

Figure 2. Compound 5 prevented glutamate and acrolein-induced HT22 cell death and upregulated the protein expression of HO-1. (A) Investigation of protection of compound **5** on HT22 cells exposed to 3 mM glutamate and 25 μM acrolein for 24 h using phase-contrast images. (B) Compound **5** didn't release LDH until 300 μM. Cell viability was tested by LDH assay. It released LDH on HT22 cells in a concentration-dependent manner. (C) Compound **5** possessed the best neuroprotective activity on glutamate and acrolein induced death on HT22 cell line. The cells were treated with 3, 10 μM of compound **5** for 30 mins before adding the toxic drugs glutamate (3 mM) and acrolein (20 μM). Cell viability was tested by MTT assay. (D) Compound **5** (10 μM) increased the evaluation of HO-1among the candidate compounds by western blot. The cells were incubated with compound **5** for 24 hours. Glu, Rol, Acr are short for glutamate, Rolipram and acrolein respectively. All data were represented as mean ± SEM from three independent experiments; $^{**}P<0.01$, $^{***}P<0.001$ versus control.

Compound 5 increased the levels of p-CREB and BDNF in HT22 cells.

Biological effects such as regeneration and differentiation are also necessary for the survival and normal physiological functions of mature central and peripheral nervous system neurons.[35,36] Previous studies have indicated that brain-derived neurotrophic factor (BDNF) plays an important role in the survival, differentiation, growth and development of neurons.[36,37] In addition, cyclic AMP response protein element binding protein (CREB) is an intranuclear transcription factor and phosphorylated CREB is associated with cell death from hypoxia tolerance. Studies showed that cerebral ischemic injury and TBI inhibited p-CREB.[38] So, the effects of compound **5** on BDNF and CREB signaling were investigated. Compound **5** significantly increased the protein levels of p-CREB and BDNF (Figure 3A, B) in HT22 cells. The results were further confirmed by the immunocytostaining in HT22 cells (Figure 3C).

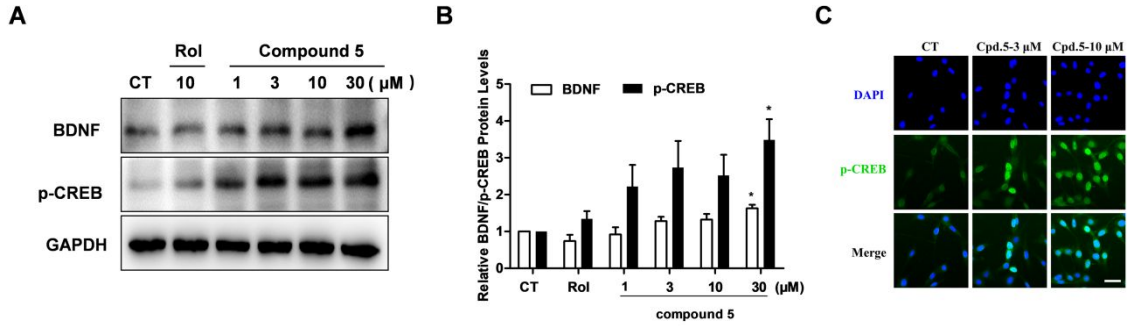

Figure 3. Compound 5 up-regulated the expression of p-CREB and BDNF in HT22 cells. (A) Compound **5** increased the protein levels of BDNF and p-CREB by western blot. HT22 cells were incubated with Rolipram (10 μM) and compound **5** (1-30 μM) for 24 h. (B) Quantitative analysis of BDNF and p-CREB protein levels. (C) Compound **5** increased the expression of p-CREB by immunofluorescence. HT22 cells were subjected to compound **5** (3-10 μM) for 24 h. Cells were dyed

for the expression of p-CREB (green). Nuclei was counterstained with DAPI (blue). Scale bar = 40 μm. One-way ANOVA with Tukey post-hoc comparisons were performed in statistical analyses. All data were represented as mean ± SEM from three independent experiments. Error bars represent the SEM. Comparisons to control indicated by $*P < 0.05$ versus control.

Compound 5 reduced the expression levels of PDE4B protein in HT22 cells.

PDE4B, one of PDE4 subtypes widely distributes in the brain and has been reported to be involved in the regulation of anti-inflammatory.[39] Drugs which could reduce PDE4B expression and stimulate the CREB pathway may enhance anti-inflammatory activities.[40] Moreover, modulate PDE4 will also increase BDNF expression.[41] We speculated that compound **5** may have similar function with Rolipram to inhibit PDE4. Firstly, the potential binding activity of compound **5** with PDE4 was predicted by using molecular docking. We found that compound **5** and Rolipram shared similar binding conformations and interactions with PDE4D activity pocket (Data were shown in supplementary information). Then, we tested the hybrids on the enzyme activities of PDE4B and PDE4D7. Unexpectedly, compound **5** had little effects on the activities of PDE4B2 and PDE4D7 (Data were shown in Supplementary information). Furtherly the protein level of PDE4B was detected. We found that compound **5** could decrease the protein level of PDE4B (Figure 4A, B). These results suggested that compound **5** could modulate PDE/CREB pathway by directly decreasing PDE4B protein rather than inhibiting its enzyme activity. It has been reported that Michael- addition- reaction- based protein degradation system can be used as a strategy to design novel drugs to modulate signaling pathway.[42,43] Compound **5** contained a benzoic

acid moiety, suggesting that it might degrade PDE4B mostly likely due to the Michael-addition- reaction- based protein degradation system. It is different from the compounds designed by PROTAC (PROteolysis Targeting Chimeras), another hot protein degradation system.[44,45] To confirm the speculation, of course, further studies should be conducted.

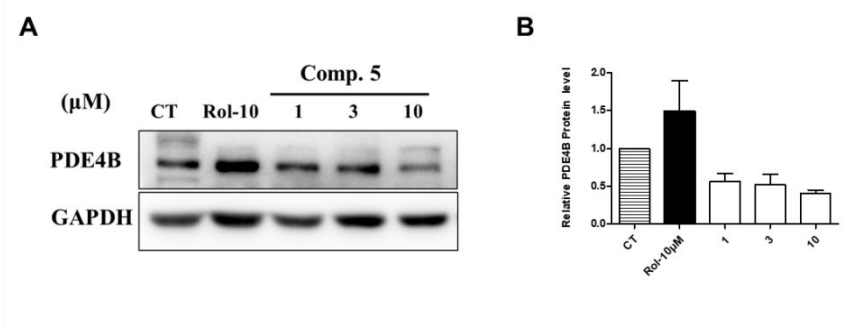

Figure 4. Compound 5 downregulated the levels of PDE4B protein in HT22 cells. (A). Compound **5** reduced PDE4B protein levels by western blot. HT22 cells were treated with Rolipram (10 μM) or different concentrations (1-30 μM) of compound **5** for 24 h. (B) Quantitative analysis of BDNF and p-CREB protein levels. All data were represented as mean ± SEM from three independent experiments.

Compound 5 attenuated lipopolysaccharide (LPS)-induced inflammation in BV2 cells.

Neuroinflammation has been closely involved in diversity of CNS diseases, including NDDs and TBI.[46] Microglia, resident macrophages in the brain, plays a pivotal role in the occurrence and development of neuroinflammation. Both acute and chronic neuroinflammation might damage the neurons. Many proinflammatory cytokines would be released by activated microglia, such as nitric oxide (NO), tumor necrosis factor (TNF-α) and interleukin 1β (IL-1β), while the pathway of the NF-κB signaling was activated and accompanied with neuroinflammation.[47,48] We explored the potential anti-inflammatory

activity of compound **5** and it reduced the elevated NO in a dose-dependent manner in BV2 cells (Figure 5A). In addition, compound **5** (10 μM) notably decreased the nuclear protein level of NF-κB and also inhibited the nuclear translocation of NF-κB, indicating that compound **5** may inhibit LPS-induced neuroinflammation through modulating the NF-κB pathway (Figure 5B, C).

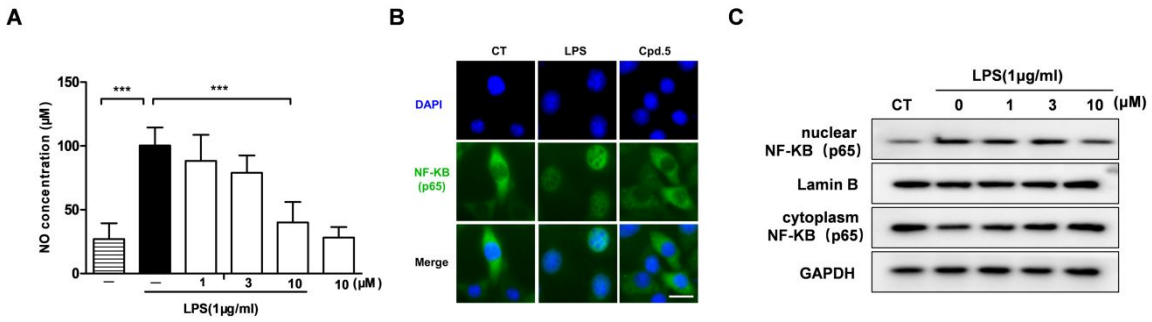

Figure 5. Compound 5 attenuated the LPS-induced inflammation in BV2 cells. (A). Compound **5** treatment reduced NO released in LPS-stimulated BV2 cells. BV2 cells were treated with 1 μg/mL of LPS alone, or with LPS plus different concentrations (1-10 μM) of compound **5** for 24 h. NO in the supernatants was determined using Griess reagent. (B) Compound **5** inhibited the nuclear translocation of NF-κB. The nuclear translocation of NF-κB was observed after incubated with LPS for 2 h and plus compound **5** of 10 μM by immunofluorescence. (C) Compound **5** reduced nuclear NF-κB p65 protein levels in LPS-stimulated BV2 cells by western blot. BV2 cells were treated with 1 μg/mL of LPS alone, or with LPS plus different concentrations (1-10 μM) of compound **5** for 2 h. All data were represented as mean ± SEM from three independent experiments; ***P<0.001 versus control.

Physicochemical properties and prediction of ADMET properties

In silico assessment of physicochemical properties and ADME predictions of the best active

compound was carried out using ACD/Percepta v14.1.0 and SwissADME.[49,50] For the most promising novel Rolipram-Tranilast hybrids, a series of ADMET properties (absorption, distribution, metabolism, excretion and toxicological properties) were calculated. In detail, we took into account the logarithmic ratio of the octanol–water partitioning coefficient (clog P), molecular weight (MW), rotatable bonds, H-bond acceptors, H-bond donors (Lipinski's Rule of Five),[51] Caco2 (derived from human colon adenocarcinoma cells) permeability, CNS penetration scores.[52,53] As shown in Table 2-1, compound **5** was predicted to reach the CNS, being characterized by adequate lipophilicity values and followed the Lipinski's rules.

Table 2-1. Physicochemical properties of compound 5

Compd.	LogP	M.W.	Rotatable bonds	H-bond acceptors	H-bond donors	Caco2 permeability (Pe)	CNS penetration (Score)
5	4.26	380.48	8	3	1	230E-6	-2.69

Note: M.W.: molecular weight; **LogP:** logarithm of the octanol-water partition coefficient;

Absorption refers to the process by which the drug can go to the systemic circulation through the organs of the body. Several routes for absorption such as oral absorption and permeability through certain cells such as Caco2 were measured. By inspecting results recorded in Table 2-2, it was found that compound **5** showed good intestinal absorption. The second property is the distribution, through which the transformation of the molecules from one tissue or organ to another can be predicted. BBB penetration was the distribution parameters used in this study, permitting the diffusion of hydrophobic and small molecules

to the brain. Results showed that compound **5** had the ability of BBB penetration. About absorption and BBB penetration of compound **5**, the predictions of the two software were consistent. It was calculated that compound **5** was able to inhibit drug metabolizing enzymes cytochrome P450 isoforms, such as CYP2C19, CYP2C9, CYP2D6 but not CYP1A2. Moreover, glycoprotein (P-gp) substrate was measured to predict excretion property. Compound **5** had no inhibitory effect on P-gp. In addition, preliminary data concerning toxicity profiles of compound **5** were predicted, in terms of calculating the median lethal dose (LD_{50}) by oral administration. Prediction of toxicological behavior indicated that compound **5** was low toxicity with LD_{50} at 300-5000 mg/Kg. From the predicted ADMET properties of the novel synthesized compound **5**, it was justified that it may have good characters as a lead compound.

Table 2-2. ADMET prediction of compound 5

Compd.	GI absorption	BBB permeant	Pgp substrate	CYP1A2 inhibitor	CYP2C19 inhibitor	CYP2C9 inhibitor	CYP2D6 inhibitor	$LD_{50}\leq$ (mg/Kg)	$LD_{50}\geq$ (mg/Kg)
5	High	Yes	No	No	Yes	Yes	Yes	5000	300

Pharmacology Evaluation In vivo

Compound 5 reduced the bleeding area and repaired the damaged BBB in a mouse model of TBI.

TBI can be caused by head hitting, skull penetration, fast acceleration or deceleration, or blasting exposure. These injuries would cause the physical, emotional, and psychosocial changes, affecting the patients' daily activities and lifespan.[54,55] Reducing neuronal death

has been considered as a fundamental therapy for TBI. It has been reported that chronic cognitive dysfunction after TBI could be improved by PDE inhibitors.[56,57] The anti-TBI effects of compound **5** were investigated in an established animal model of TBI by air pistol as reported before (Figure 6A, B).[58] We found that compound **5** significantly decreased the hemorrhagic area in a dosage-dependent manner in TBI mice (Figure 6C, D). BBB disruption has been recognized as important pathological processes in early stage of TBI. BBB permeability was evaluated by EB extravasation using spectrophotometry as previously described.[59,60] Compound **5** effectively attenuated the EB leakage induced by TBI (Figure 6E). Moreover, matrix metalloproteinases (MMPs) are a series of proteinases which can reflect the function of BBB, especially MMP2 and MMP9.[61] Compound **5** could reduce the protein levels of MMP2 and MMP9 after TBI(Figure 6G, F). These data demonstrated that compound **5** attenuated the BBB disruption after TBI.

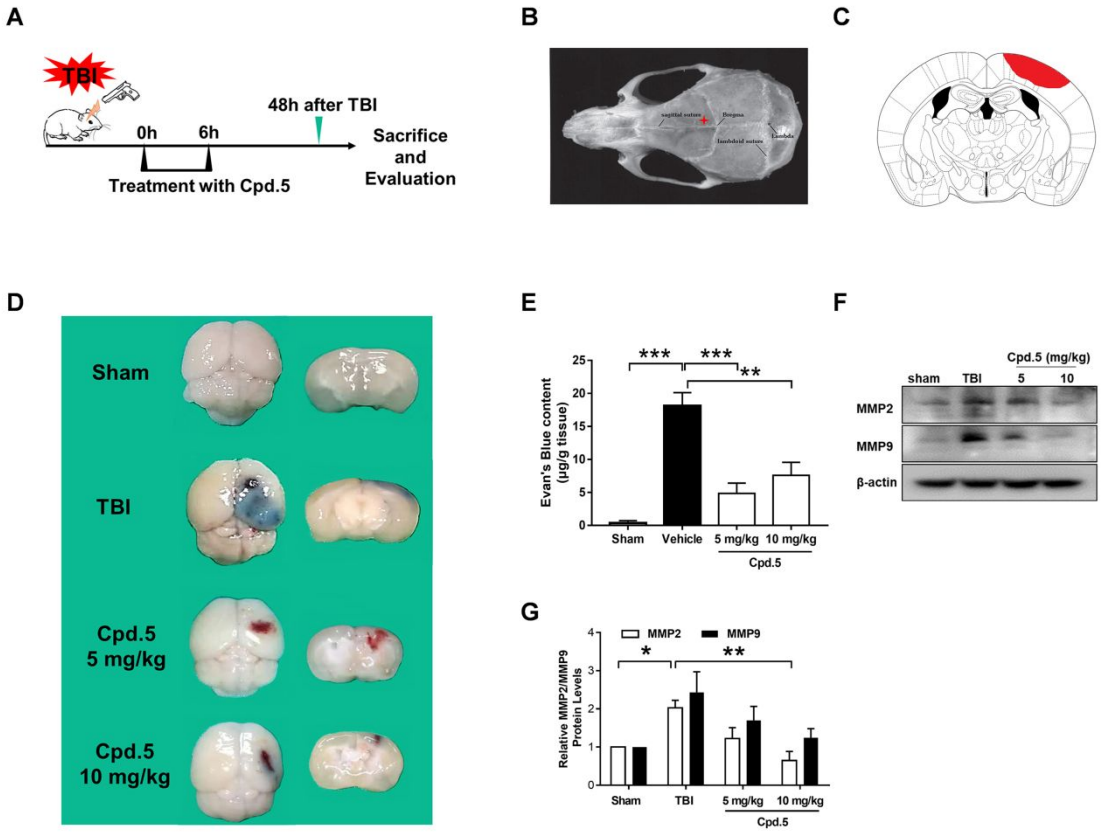

Figure 6. Compound 5 showed anti-ischemic activity and neuroprotection of BBB in TBI mice. Compound **5** was administered by gavage in two divided doses, and was administered at 0 h and 6 h after awaking. (A) The time line and sketch map of the establishment of animal model of TBI. (B, C) General strike position was showed in the anatomy map. (D) Compound **5** decreased the ischemic area of TBI through dissection visually. (E) Compound **5** could protect the broken brain blood barrier of TBI by Evans blue tests. (F) Compound **5** reduced MMP2 and MMP9 protein levels in TBI animal models by western blot. (G) Quantitative analysis of (F). All data were represented as mean ± SEM from three independent experiments; *P<0.05, **P<0.01, ***P<0.001 versus control.

5. Conclusion

In this study, we designed and synthesized a series of novel Rolipram-Tranilast hybrids bearing cyclopentane moiety and evaluated neuroprotective activity in vitro and in vivo. Among these chemicals, compound **5** protected against the glutamate- and acrolein-induced cell death in HT22 cells and increased the expression of BDNF and p-CREB. Furthermore, compound **5** suppressed the neuroinflammation by reducing LPS-induced NO release and inhibits nuclear translocation of NF-κB. Finally, compound **5** significantly reduced the bleeding area and repaired the damaged BBB in a mouse model of TBI. Taken together, our findings demonstrated that compound **5** might be a novel multifunctional neuroprotective agent for the treatment of TBI or other NNDs.

Experimental section

1. Chemistry

Unless otherwise stated, all the reagents and solvents were purchased from commercial

sources and were used without further purification. Thin-layer chromatography (TLC) was used to monitor the reactions by E. Merck silica-gel 60 F254 precoated plates (GF_{254}). Flash chromatography was performed with silica gel (200-300 mesh) purchased from Qingdao Haiyang Chemical Co. Ltd. The ^{1}H and ^{13}C nuclear magnetic resonance (NMR) spectra were recorded on a Bruker Avance spectrometer 400 at 400 and 100 MHz, respectively. Chemical shifts are given in ppm (δ) referenced to $CDCl_3$ with 7.26 for ^{1}H and 77.16 for ^{13}C, and to DMSO- d_6 with 2.50 for ^{1}H and 39.52 for ^{13}C. In the case of multiplet, the signals are reported as intervals. Signals are abbreviated as follows: s, singlet; d, doublet; t, triplet; q, quartet; m, multiplet and dd, doublet of doublets. Coupling constants are expressed in hertz. High-resolution mass spectrometric data (HRMS) were collected on a Shimadzu LCMS-IT-TOF mass spectrometer.

*1.1 Synthesis of ethyl (E)-3-(4-hydroxy-3-methoxyphenyl) acrylate (**2a**)*

To a solution of 4-hydroxy-3-methoxycinnamic acid (**1a**) (10.00 g, 52 mmol) in anhydrous ethanol (100 mL), concentrated sulfuric acid (0.5 mL) was added. The reaction mixture was refluxed overnight. The reaction was monitored by TLC, after finishing, the solvent was removed in vacuo, the residue was dissolved in ethyl acetate (300 mL), washed with saturated aq. $NaHCO_3$ followed with brine, dried with anhydrous Na_2SO_4, concentration afforded **2a** as a white solid (10.53 g, yield 92 %). ^{1}H NMR (400 MHz, Chloroform-*d*) δ 7.61 (d, J = 15.9 Hz, 1H), 7.12 – 7.00 (m, 2H), 6.92 (d, J = 8.2 Hz, 1H), 6.29 (d, J = 15.9 Hz, 1H), 5.92 (s, 1H), 4.26 (q, J = 7.1 Hz, 2H), 3.92 (s, 3H), 1.33 (t, J = 7.1 Hz, 3H).

*1.2 Synthesis of ethyl (E)-3-(3-hydroxy-4-methoxyphenyl) acrylate (**2b**)*

The procedure was similar to the preparation of **2a, 2b** as a white solid (10.85 g, yield 95 %). ^{1}H NMR (400 MHz, $CDCl_3$) δ 7.56 (d, *J* = 15.9 Hz, 1H), 7.10 (d, *J* = 2.1 Hz, 1H), 6.98 (dd, *J* = 8.3, 2.1 Hz, 1H), 6.80 (d, *J* = 8.3 Hz, 1H), 6.25 (d, *J* = 15.9 Hz, 1H), 5.86 (s, 1H), 4.22 (q, *J* = 7.1 Hz, 2H), 3.87 (s, 3H), 1.29 (t, *J* = 7.1 Hz, 3H). ^{13}C NMR (100MHz, $CDCl_3$) δ 167.54, 148.73, 146.03, 144.64, 128.20, 121.92, 116.37, 113.23, 110.72, 60.55, 56.12, 14.48.

*1.3 Synthesis of ethyl (E)-3-(4-(cyclopentyloxy)-3-methoxyphenyl) acrylate (**3a**)*

To a solution of **2a** (10.00 g, 45 mmol) in DMF (60 mL), K_2CO_3 (9.33 g, 68 mmol) and KI (224 mg, 1.35 mmol) were added. After stirring at 80 °C for 2 h, bromocyclopentane (6.3 mL, 59 mmol) was added dropwise at 65 °C. Then the reaction mixture was stirred at 65 °C for 24 h. After completion of the reaction, as indicated by TLC, the solvent was removed in vacuo. The residue was dissolved in water (200 mL) and then extracted with ethyl acetate 200 mL three times. The combined organic phase was washed with brine, dried with anhydrous Na_2SO_4, concentrated, and purified by column chromatography over silica gel (20:1, petroleum ether/ ethyl acetate) to give **3a** as a white solid (8.75 g, yield 67 %). ^{1}H NMR (400 MHz, Chloroform-*d*) *δ* 7.62 (d, *J* = 15.9 Hz, 1H), 7.09 – 7.03 (m, 2H), 6.85 (d, *J* = 8.2 Hz, 1H), 6.29 (d, *J* = 15.9 Hz, 1H), 4.80 (tt, *J* = 6.4, 3.2 Hz, 1H), 4.25 (q, *J* = 7.1 Hz, 2H), 3.87 (s, 3H), 2.03 – 1.77 (m, 6H), 1.62 (dq, *J* = 12.3, 6.8, 5.9 Hz, 2H), 1.33 (t, *J* = 7.1 Hz, 3H).

*1.4 Synthesis of ethyl (E)-3-(3-(cyclopentyloxy)-4-methoxyphenyl) acrylate (**3b**)*

The procedure was similar to the preparation of **3a**, **3b** as a white solid (9.01 g, yield 65 %). ^{1}H NMR (400 MHz, Chloroform-*d*) *δ* 7.62 (d, *J* = 15.9 Hz, 1H), 7.10 – 7.04 (m, 2H), 6.85

(d, J = 8.1 Hz, 1H), 6.28 (d, J = 15.9 Hz, 1H), 4.79 (tt, J = 6.5, 3.1 Hz, 1H), 4.26 (q, J = 7.1 Hz, 2H), 3.87 (s, 3H), 2.01 – 1.80 (m, 6H), 1.63 (dq, J = 12.5, 4.0 Hz, 2H), 1.33 (t, J = 7.1 Hz, 3H).

*1.5 Synthesis of (E)-3-(4-(cyclopentyloxy)-3-methoxyphenyl) acrylic acid (**4a**)*

To a solution of **3a** (8.00 g, 28 mmol) in THF (80 mL), 2N aq. NaOH (200 mL) was added. The reaction mixture was stirred at 80 °C overnight. After completion of the reaction, as indicated by TLC, the THF was removed by rotary evaporation. The pH of the remaining liquid was adjusted to 2 by concentrated hydrochloric acid. Then the product was extracted with ethyl acetate (50 mL × 3). The combined organic phase was washed with brine, dried with anhydrous Na_2SO_4, filtered, and evaporated under reduced pressure to give **4a** as a white solid (6,000 mg, 83 %). ^{1}H NMR (400 MHz, Chloroform-*d*) δ 7.73 (d, J = 15.9 Hz, 1H), 7.15 – 7.05 (m, 2H), 6.87 (d, J = 8.3 Hz, 1H), 6.30 (d, J = 15.9 Hz, 1H), 4.80 (dq, J = 6.4, 3.1 Hz, 1H), 3.88 (s, 3H), 2.01 – 1.81 (m, 6H), 1.64 (tq, J = 12.5, 7.3, 5.2 Hz, 2H).

*1.6 Synthesis of (E)-3-(3-(cyclopentyloxy)-4-methoxyphenyl) acrylic acid (**4b**)*

To a solution of **3b** (9.01 g, 31 mmol) in THF (90 mL), 2N aq. NaOH (230 mL) was added. The reaction mixture was stirred at 80 °C overnight. After completion of the reaction, as indicated by TLC, the THF was removed by rotary evaporation. The pH of the remaining liquid was adjusted to 2 by concentrated hydrochloric acid. Then the product was extracted with ethyl acetate (50 mL × 3). The combined organic phase was washed with brine, dried with anhydrous Na_2SO_4, filtered, and evaporated under reduced pressure to give **4b** as a white solid (7.27 g, yield 89 %). ^{1}H NMR (400 MHz, Chloroform-*d*) δ 7.73 (d, J = 15.9 Hz,

1H), 7.15 – 7.05 (m, 2H), 6.87 (d, J = 8.3 Hz, 1H), 6.30 (d, J = 15.9 Hz, 1H), 4.80 (dq, J = 6.4, 3.1 Hz, 1H), 3.88 (s, 3H), 2.01 – 1.81 (m, 6H), 1.64 (tq, J = 12.5, 7.3, 5.2 Hz, 2H).

2 Synthesis procedure for compounds 3-26

*(E)-3-(4-(cyclopentyloxy)-3-methoxyphenyl)-N-(2-hydroxyphenyl)acrylamide (**3**)*

To a solution of **4a** (120 mg, 0.46 mmol), 2-aminophenol (100 mg, 0.92 mmol), HOBT (93 mg, 0.69 mmol) and EDCI (132 mg, 0.69 mmol) in anhydrous DCM (5 mL), Et_3N (191 μL, 1.38 mmol) was added. The reaction mixture was stirred at RT overnight. After completion of the reaction, as indicated by TLC, DCM (10 mL) was added. Then the reaction mixture was washed with saturated aq. $NaHCO_3$ (15 mL × 2) and brine, dried with anhydrous Na_2SO_4, filtered, evaporated under reduced pressure, and purified by column chromatography over silica gel (1:2, petroleum ether/ DCM, v/v) to give **3** as a yellow solid (54 mg, 33 %). ^{1}H NMR (400 MHz, Chloroform-*d*) δ 9.42 (s, 1H), 7.77 – 7.68 (m, 2H), 7.18 – 6.99 (m, 5H), 6.90 – 6.80 (m, 2H), 6.48 (d, J = 15.3 Hz, 1H), 4.81 (tt, J = 6.4, 3.2 Hz, 1H), 3.86 (s, 3H), 2.02 – 1.76 (m, 6H), 1.63 (qd, J = 5.2, 2.2 Hz, 2H). ^{13}C NMR (100 MHz, Chloroform-*d*) δ 166.01, 150.20, 149.95, 149.08, 144.28, 127.28, 126.73, 125.82, 122.69, 122.21, 120.38, 120.03, 116.08, 114.03, 110.70, 80.52, 56.07, 32.88, 24.15. HRMS (ESI) *m/z* calcd for $C_{21}H_{23}NO_4$ $[M+H]^+$: 354.1627; Found: 354.1639.

*(E)-3-(3-(cyclopentyloxy)-4-methoxyphenyl)-N-(2-hydroxyphenyl)acrylamide (**15**)*

To a solution of **4b** (223 mg, 0.85 mmol), 2-aminophenol (185 mg, 1.70 mmol), HOBT (170 mg, 1.26 mmol) and EDCI (244 mg, 1.26 mmol) in anhydrous DCM (8 mL), Et_3N (353 μL,

2.55 mmol) was added. The reaction mixture was stirred at RT overnight. After completion of the reaction, as indicated by TLC, DCM (10 mL) was added. Then the reaction mixture was washed with saturated aq. $NaHCO_3$ (15 mL × 2) and brine, dried with anhydrous Na_2SO_4, filtered, evaporated under reduced pressure, and purified by column chromatography over silica gel (3:4, petroleum ether/ DCM, v/v) to give **15** as a yellow solid (100 mg, 33 %). [**15**]^{1}H-NMR (400 MHz, Chloroform-*d*) δ 9.56 (s, 1H), 8.09 (s, 1H), 7.73 (d, J = 15.4 Hz, 1H), 7.19 – 7.01 (m, 5H), 6.92 – 6.79 (m, 2H), 6.53 (d, J = 15.4 Hz, 1H), 4.79 (tt, J = 6.2, 3.3 Hz, 1H), 3.88 (s, 3H), 2.00 – 1.80 (m, 6H), 1.69 – 1.54 (m, 2H). ^{13}C NMR (100 MHz, Chloroform-*d*) δ 166.05, 152.18, 148.89, 147.74, 144.10, 127.14, 127.11, 125.93, 122.29, 122.24, 120.41, 119.75, 116.42, 113.82, 111.69, 80.68, 55.99, 32.81, 24.08. HRMS (ESI) *m/z* calcd for $C_{21}H_{23}NO_4$ $[M+H]^+$: 354.1627; Found: 354.1634.

*(E)-3-(4-(cyclopentyloxy)-3-methoxyphenyl)-N-(3-(trifluoromethyl) phenyl) acrylamide (**4**)*

Yellow solid (yield:44 %). ^{1}H NMR (400 MHz, Chloroform-*d*) δ 8.00 (s, 1H), 7.93 (s, 1H), 7.87 (d, J = 8.2 Hz, 1H), 7.70 (d, J = 15.4 Hz, 1H), 7.43 (t, J = 8.0 Hz, 1H), 7.35 (d, J = 7.8 Hz, 1H), 7.04 (d, J = 8.3 Hz, 1H), 7.00 (s, 1H), 6.82 (d, J = 8.3 Hz, 1H), 6.45 (d, J = 15.4 Hz, 1H), 4.79 (tt, J = 6.1, 2.8 Hz, 1H), 3.80 (s, 3H), 1.97 – 1.79 (m, 6H), 1.65 – 1.57 (m, 2H). ^{13}C NMR (100MHz, Chloroform-*d*) δ 164.73, 149.89, 143.08, 138.85, 131.53, 131.21, 129.57, 127.01, 125.22, 122.90, 122.32, 117.81, 116.55, 114.05, 110.67, 80.51, 55.96, 32.86, 24.13. HRMS (ESI) *m/z* calcd for $C_{22}H_{22}F_3NO_3$ $[M+H]^+$: 406.1552; Found: 406.1537.

*(E)-3-(3-(cyclopentyloxy)-4-methoxyphenyl)-N-(3-(trifluoromethyl) phenyl) acrylamide (**16**)*

Yellow solid (yield: 52 %). ^{1}H NMR (400 MHz, Chloroform-d) δ 8.01 (s, 1H), 7.92 (s, 1H), 7.88 (d, J = 8.2 Hz, 1H), 7.70 (d, J = 15.5 Hz, 1H), 7.43 (t, J = 7.9 Hz, 1H), 7.35 (d, J = 7.8 Hz, 1H), 7.05 (d, J = 7.4 Hz, 2H), 6.85 – 6.79 (m, 1H), 6.45 (d, J = 15.4 Hz, 1H), 4.76 (tt, J = 5.8, 3.5 Hz, 1H), 3.85 (s, 3H), 1.94 – 1.86 (m, 4H), 1.85 – 1.78 (m, 2H), 1.59 (m, 2H). ^{13}C NMR (100 MHz, Chloroform-*d*) δ 163.69, 151.03, 146.66, 142.08, 137.80, 130.49, 130.16, 128.54, 126.26, 124.19, 121.88, 121.14, 119.66, 116.87, 115.52, 112.82, 110.65, 79.73, 54.93, 31.76, 23.02. HRMS (ESI) *m/z* calcd for $C_{22}H_{22}F_3NO_3$ $[M+H]^+$: 406.1552; Found: 406.1543.

*(E)-3-(4-(cyclopentyloxy)-3-methoxyphenyl)-N-(4-(dimethylamino) phenyl) acrylamide (**5**)*

Yellow solid (yield: 47 %). ^{1}H NMR (400 MHz, Chloroform-*d*) δ 7.65 (d, J = 15.4 Hz, 1H), 7.49 (d, J = 8.5 Hz, 2H), 7.43 (s, 1H), 7.11 – 6.98 (m, 2H), 6.83 (d, J = 8.3 Hz, 1H), 6.74 (d, J = 8.5 Hz, 2H), 6.42 (d, J = 15.4 Hz, 1H), 4.79 (tt, J = 6.4, 3.2 Hz, 1H), 3.84 (s, 3H), 2.92 (s, 6H), 2.00 – 1.78 (m, 6H), 1.69 – 1.54 (m, 2H). ^{13}C NMR (100 MHz, Chloroform-*d*) δ 163.00, 148.90, 148.48, 140.39, 126.50, 120.94, 120.55, 117.77, 113.14, 112.30, 109.52, 79.41, 55.01, 40.07, 31.85, 23.10. HRMS (ESI) *m/z* calcd for $C_{23}H_{28}N_2O_3$ $[M+H]^+$: 381.2100; Found: 381.2116.

*(E)-3-(3-(cyclopentyloxy)-4-methoxyphenyl)-N-(4-(dimethylamino) phenyl) acrylamide (**17**)*

Yellow solid (yield: 37 %). ^{1}H NMR (400 MHz, Chloroform-*d*) δ 7.66 (s, 1H), 7.53 (s, 1H), 7.49 (d, J = 8.4 Hz, 2H), 7.10 – 6.99 (m, 2H), 6.82 (d, J = 8.2 Hz, 1H), 6.71 (d, J = 8.9 Hz, 2H), 6.42 (d, J = 15.4 Hz, 1H), 4.76 (s, 1H), 3.85 (s, 3H), 2.91 (s, 6H), 1.96 – 1.76 (m, 6H), 1.68 – 1.53 (m, 2H). ^{13}C NMR (100 MHz, Chloroform-*d*) δ 164.07, 151.63, 147.76, 141.37,

127.82, 121.59, 119.02, 113.77, 113.15, 111.74, 80.58, 56.02, 40.96, 32.83, 24.09. HRMS (ESI) *m/z* calcd for $C_{23}H_{28}N_2O_3$ $[M+H]^+$: 381.2100; Found: 381.2122.

*(E)-3-(4-(cyclopentyloxy)-3-methoxyphenyl)-N-phenylacrylamide (**6**)*

White solid (yield: 46%). ^{1}H NMR (400 MHz, Chloroform-*d*) δ 7.72 – 7.59 (m, 4H), 7.36 – 7.29 (m, 2H), 7.14 – 7.08 (m, 1H), 7.05 (dd, J = 8.3, 2.1 Hz, 1H), 7.01 (d, J = 2.1 Hz, 1H), 6.82 (d, J = 8.3 Hz, 1H), 6.45 (d, J = 15.4 Hz, 1H), 4.79 (tt, J = 6.4, 3.2 Hz, 1H), 3.82 (s, 3H), 2.02 – 1.75 (m, 6H), 1.61 (dtd, J = 6.9, 5.2, 3.2 Hz, 2H). ^{13}C NMR (100 MHz, Chloroform-*d*) δ 164.46, 149.91, 149.70, 142.34, 138.27, 129.05, 127.25, 124.26, 122.15, 118.42, 118.40, 114.10, 110.60, 80.47, 55.99, 32.88, 24.14. HRMS (ESI) *m/z* calcd for $C_{21}H_{23}NO_3$ $[M+H]^+$: 338.1678; Found: 338.1685.

*(E)-3-(3-(cyclopentyloxy)-4-methoxyphenyl)-N-phenylacrylamide (**18**)*

White solid (yield: 51 %). ^{1}H NMR (400 MHz, Chloroform-*d*) δ 7.78 (s, 1H), 7.71 – 7.60 (m, 3H), 7.36 – 7.29 (m, 2H), 7.14 – 7.07 (m, 1H), 7.07 – 7.01 (m, 2H), 6.81 (d, J = 8.3 Hz, 1H), 6.46 (d, J = 15.5 Hz, 1H), 4.74 (tt, J = 5.9, 3.5 Hz, 1H), 3.85 (s, 3H), 1.75 – 1.96 (m, 6H), 1.65 – 1.53 (m, 2H). ^{13}C NMR (100 MHz, Chloroform-*d*) δ 164.51, 151.78, 147.74, 142.34, 138.29, 129.05, 127.54, 124.25, 121.81, 119.93, 118.57, 113.71, 111.68, 80.58, 55.99, 32.82, 24.09. HRMS (ESI) *m/z* calcd for $C_{21}H_{23}NO_3$ $[M+H]^+$: 338.1678; Found: 338.1696.

(E)-3-(4-(cyclopentyloxy)-3-methoxyphenyl)-N-(4-(trifluoromethyl) phenyl) acrylamide (7)

White solid (yield: 64 %). ^{1}H NMR (400 MHz, Chloroform-d) δ 7.75 (d, J = 8.4 Hz, 2H),

7.71 (d, *J* = 15.4 Hz, 1H), 7.64 (s, 1H), 7.59 (d, *J* = 8.4 Hz, 2H), 7.08 (dd, *J* = 8.3, 2.0 Hz, 1H), 7.03 (d, *J* = 2.0 Hz, 1H), 6.85 (d, *J* = 8.3 Hz, 1H), 6.42 (d, *J* = 15.4 Hz, 1H), 4.81 (tt, *J* = 6.4, 3.2 Hz, 1H), 3.85 (s, 3H), 2.03 – 1.76 (m, 6H), 1.65 – 1.59 (m, 2H). ^{13}C NMR (100 MHz, Chloroform-*d*) δ 164.51, 150.05, 149.96, 143.39, 141.29, 126.91, 126.38, 126.34, 126.30, 126.26, 122.43, 119.38, 117.62, 114.07, 110.64, 80.51, 56.04, 32.88, 24.14. HRMS (ESI) *m/z* calcd for $C_{22}H_{22}F_3NO_3$ $[M+H]^+$: 406.1552; Found: 406.1535.

*(E)-3-(3-(cyclopentyloxy)-4-methoxyphenyl)-N-(4-(trifluoromethyl) phenyl) acrylamide (**19**)*

White solid (yield: 34 %). ^{1}H NMR (400 MHz, Chloroform-*d*) δ 10.46 (s, 1H), 7.91 (d, *J* = 8.5 Hz, 2H), 7.70 (d, *J* = 8.6 Hz, 2H), 7.58 (d, *J* = 15.6 Hz, 1H), 7.25 – 7.17 (m, 2H), 7.02 (d, *J* = 8.9 Hz, 1H), 6.70 (d, *J* = 15.6 Hz, 1H), 4.85 (tt, *J* = 5.9, 2.6 Hz, 1H), 3.80 (s, 3H), 1.94 (dp, *J* = 11.9, 8.1, 6.3 Hz, 2H), 1.81 – 1.68 (m, 4H), 1.66 – 1.54 (m, 2H). ^{13}C NMR (100 MHz, Chloroform-*d*) δ 164.83, 151.90, 147.62, 143.45, 141.78, 127.67, 126.63, 126.59, 126.55, 126.51, 122.28, 119.64, 119.44, 113.63, 112.65, 80.01, 56.06, 32.75, 24.09. HRMS (ESI) *m/z* calcd for $C_{22}H_{22}F_3NO_3$ $[M+H]^+$: 406.1552; Found: 406.1547.

*(E)-N-(4-aminophenyl)-3-(4-(cyclopentyloxy)-3-methoxyphenyl) acrylamide (**8**)*

Yellow solid (yield: 50 %). ^{1}H NMR (400 MHz, Chloroform-*d*) δ 9.71 (s, 1H), 7.43 (d, *J* = 15.6 Hz, 1H), 7.36 (dd, *J* = 8.7, 1.8 Hz, 2H), 7.17 (d, *J* = 2.0 Hz, 1H), 7.12 (dd, *J* = 8.3, 2.0 Hz, 1H), 6.96 (d, *J* = 8.3 Hz, 1H), 6.65 (d, *J* = 15.6 Hz, 1H), 6.57 – 6.50 (m, 2H), 4.82 (tt, *J* = 6.1, 2.6 Hz, 1H), 3.80 (s, 3H), 3.35 (s, 2H), 1.97 – 1.83 (m, 2H), 1.77 – 1.64 (m, 4H), 1.57 (qt, *J* = 6.3, 3.1 Hz, 2H). ^{13}C NMR (100 MHz, Chloroform-*d*) δ 163.38, 150.05, 148.93, 145.21, 139.45, 129.20, 128.01, 121.84, 121.11, 121.02, 120.76, 114.71, 114.33, 110.81,

79.95, 55.89, 32.77, 24.13. HRMS (ESI) *m/z* calcd for $C_{21}H_{24}N_2O_3$ $[M+H]^+$: 353.1787; Found: 353.1776.

*(E)-N-(4-aminophenyl)-3-(3-(cyclopentyloxy)-4-methoxyphenyl) acrylamide (**20**)*

Yellow solid (yield: 51 %). ^{1}H NMR (400 MHz, Chloroform-*d*) δ 7.63 (d, J = 15.4 Hz, 1H), 7.47 (s, 1H), 7.39 (d, J = 8.2 Hz, 2H), 7.05 (dd, J = 11.3, 3.4 Hz, 2H), 6.82 (d, J = 8.2 Hz, 1H), 6.65 (d, J = 8.7 Hz, 2H), 6.39 (d, J = 15.4 Hz, 1H), 4.76 (dq, J = 6.6, 3.6, 3.1 Hz, 1H), 3.85 (s, 3H), 3.60 (s, 2H), 1.94-1.77 (m, 6H), 1.56-1.64 (m, 2H). ^{13}C NMR (100 MHz, Chloroform-*d*) δ 164.10, 151.68, 147.75, 143.25, 141.55, 129.69, 127.74, 121.82, 121.65, 118.88, 115.45, 113.77, 111.74, 80.60, 56.01, 32.82, 24.08. HRMS (ESI) *m/z* calcd for $C_{21}H_{24}N_2O_3$ $[M+H]^+$: 353.1787; Found: 353.1781.

*(E)-N-(2-aminophenyl)-3-(4-(cyclopentyloxy)-3-methoxyphenyl) acrylamide (**9**)*

Yellow solid (yield: 43 %). ^{1}H NMR (400 MHz, Chloroform-*d*) δ 7.67 (d, J = 15.4 Hz, 1H), 7.46 (s, 1H), 7.28 (s, 1H), 7.10 – 6.99 (m, 3H), 6.87 – 6.76 (m, 3H), 6.71 (s, 1H), 6.46 (d, J = 15.6 Hz, 1H), 4.80 (tt, J = 6.8, 3.3 Hz, 1H), 3.88 – 3.83 (m, 3H), 1.99 – 1.80 (m, 6H), 1.66 – 1.58 (m, 2H). ^{13}C NMR (100 MHz, Chloroform-*d*) δ 164.62, 149.95, 149.76, 142.42, 140.71, 127.22, 127.05, 125.03, 122.15, 120.28, 119.60, 118.27, 117.70, 116.75, 114.13, 110.66, 80.46, 56.09, 32.88, 24.15. HRMS (ESI) *m/z* calcd for $C_{21}H_{24}N_2O_3$ $[M+H]^+$: 353.1787; Found: 353.1796.

*(E)-N-(2-aminophenyl)-3-(3-(cyclopentyloxy)-4-methoxyphenyl) acrylamide (**21**)*

Yellow solid (yield: 46 %). ^{1}H NMR (400 MHz, Chloroform-*d*) δ 7.67 (d, J = 15.4 Hz, 1H),

7.41 (s, 1H), 7.27 (d, *J* = 8.6 Hz, 1H), 7.13 – 6.99 (m, 3H), 6.83 (dd, *J* = 12.0, 7.8 Hz, 3H), 6.44 (d, *J* = 15.5 Hz, 1H), 4.79 (d, *J* = 6.3 Hz, 1H), 3.93 (s, 2H), 3.87 (s, 3H), 2.01 – 1.77 (m, 6H), 1.66 – 1.58 (m, 2H). ^{13}C NMR (100 MHz, Chloroform-*d*) δ 151.93, 147.81, 142.51, 127.51, 127.08, 121.85, 119.62, 118.27, 117.81, 113.85, 111.74, 80.63, 56.04, 32.83, 24.07. HRMS (ESI) *m/z* calcd for $C_{21}H_{24}N_2O_3$ $[M+H]^+$: 353.1787; Found: 353.1775.

*(E)-N-(2-amino-4-fluorophenyl)-3-(4-(cyclopentyloxy)-3-methoxyphenyl) acrylamide (**10**)*

Yellow solid (yield: 39 %). ^{1}H NMR (400 MHz, Chloroform-*d*) δ 7.67 (d, *J* = 15.5 Hz, 1H), 7.18 – 6.96 (m, 3H), 6.85 (d, *J* = 8.2 Hz, 1H), 6.55 – 6.38 (m, 3H), 4.81 (dp, *J* = 6.8, 3.2 Hz, 1H), 4.05 (s, 2H), 3.86 (s, 3H), 2.06 – 1.77 (m, 6H), 1.62 (d, *J* = 4.9 Hz, 2H). ^{13}C NMR (100 MHz, Chloroform-*d*) δ 149.96, 149.87, 142.71, 135.09, 127.06, 122.19, 117.26, 117.05, 114.11, 110.66, 80.47, 56.10, 32.88, 24.15. HRMS (ESI) *m/z* calcd for $C_{21}H_{23}FN_2O_3$ $[M+H]^+$: 371.1693; Found: 371.1711.

*(E)-N-(2-amino-4-fluorophenyl)-3-(3-(cyclopentyloxy)-4-methoxyphenyl) acrylamide (**22**)*

Yellow solid (yield: 47 %). ^{1}H NMR (400 MHz, Chloroform-*d*) δ 7.89 (s, 1H), 7.66 – 7.57 (m, 1H), 7.08 (dd, *J* = 8.6, 5.9 Hz, 1H), 7.00 (d, *J* = 8.3 Hz, 2H), 6.77 (d, *J* = 8.2 Hz, 1H), 6.53 – 6.35 (m, 3H), 4.73 (tt, *J* = 6.6, 3.3 Hz, 1H), 4.07 (s, 2H), 3.83 (s, 3H), 1.95 – 1.84 (m, 4H), 1.83 – 1.74 (m, 2H), 1.58 (ttd, *J* = 7.9, 5.0, 4.0, 1.6 Hz, 2H). ^{13}C NMR (100 MHz, Chloroform-*d*) δ 165.27, 162.96, 160.54, 151.80, 147.67, 143.23, 143.12, 142.36, 127.40, 127.15, 127.05, 121.60, 119.82, 117.72, 113.98, 111.67, 105.54, 105.31, 104.06, 103.81, 80.58, 55.95, 32.78, 24.06. HRMS (ESI) *m/z* calcd for $C_{21}H_{23}FN_2O_3$ $[M+H]^+$: 371.1693; Found: 371.1704.

*(E)-3-(4-(cyclopentyloxy)-3-methoxyphenyl)-N-(pyridin-4-yl) acrylamide (**11**)*

Yellow solid (yield: 55 %). ^{1}H NMR (400 MHz, Chloroform-*d*) δ 9.09 (s, 1H), 8.53 – 8.47 (m, 2H), 7.71 (d, *J* = 15.4 Hz, 1H), 7.68 – 7.64 (m, 2H), 7.02 (dd, *J* = 8.3, 2.1 Hz, 1H), 6.95 (d, *J* = 2.1 Hz, 1H), 6.82 (d, *J* = 8.4 Hz, 1H), 6.49 (d, *J* = 15.5 Hz, 1H), 4.79 (tt, *J* = 6.4, 3.2 Hz, 1H), 3.77 (s, 3H), 1.99 – 1.91 (m, 2H), 1.91 – 1.83 (m, 2H), 1.83 – 1.75 (m, 2H), 1.64 – 1.56 (m, 2H). ^{13}C NMR (100 MHz, Chloroform-*d*) δ 165.39, 150.39, 150.01, 149.81, 146.07, 143.64, 126.86, 122.46, 117.59, 113.97, 113.83, 110.56, 80.50, 55.91, 32.85, 24.13. HRMS (ESI) *m/z* calcd for $C_{20}H_{22}N_2O_3$ $[M+H]^+$: 339.1630; Found: 339.1639.

*(E)-3-(3-(cyclopentyloxy)-4-methoxyphenyl)-N-(pyridin-4-yl) acrylamide (**23**)*

Yellow solid (yield: 61 %). ^{1}H NMR (400 MHz, Chloroform-*d*) δ 9.59 (s, 1H), 8.50 – 8.41 (m, 2H), 7.78 – 7.66 (m, 3H), 7.04 (dd, *J* = 8.4, 2.0 Hz, 1H), 7.00 (d, *J* = 2.0 Hz, 1H), 6.80 (d, *J* = 8.4 Hz, 1H), 6.60 (d, *J* = 15.5 Hz, 1H), 4.70 (ddd, *J* = 7.0, 5.7, 3.4 Hz, 1H), 3.83 (s, 3H), 1.94 – 1.68 (m, 6H), 1.61 – 1.50 (m, 2H). ^{13}C NMR (100 MHz, Chloroform-*d*) δ 165.63, 152.11, 149.58, 147.69, 147.26, 143.86, 127.18, 122.23, 117.73, 114.14, 113.66, 111.67, 80.63, 55.96, 32.78, 24.08. HRMS (ESI) *m/z* calcd for $C_{20}H_{22}N_2O_3$ $[M+H]^+$: 339.1630; Found: 339.1642.

*(E)-N-(4'-amino-[1,1'-biphenyl]-4-yl)-3-(4-(cyclopentyloxy)-3-methoxyphenyl) acrylamide (**12**)*

Yellow solid (yield: 32 %). ^{1}H NMR (400 MHz, Chloroform-*d*) δ 10.12 (s, 1H), 7.71 (d, *J* = 8.3 Hz, 2H), 7.57 – 7.47 (m, 3H), 7.38 – 7.31 (m, 2H), 7.21 (d, *J* = 2.0 Hz, 1H), 7.16 (dd,

J = 8.4, 2.0 Hz, 1H), 6.98 (d, *J* = 8.4 Hz, 1H), 6.71 (d, *J* = 15.6 Hz, 1H), 6.66 – 6.60 (m, 2H), 5.18 (s, 2H), 4.84 (tt, *J* = 6.1, 2.5 Hz, 1H), 3.81 (s, 3H), 2.00 – 1.83 (m, 2H), 1.79 – 1.65 (m, 4H), 1.65 – 1.51 (m, 2H). ^{13}C NMR (100 MHz, Chloroform-*d*) *δ* 164.14, 150.06, 149.17, 148.50, 140.58, 137.82, 136.11, 127.79, 127.60, 127.22, 125.98, 122.16, 120.27, 119.92, 114.70, 114.66, 110.86, 79.96, 55.91, 32.78, 24.14. HRMS (ESI) *m/z* calcd for $C_{27}H_{28}N_2O_3$ $[M+H]^+$: 429.2100; Found: 429.2123.

(E)-N-(4'-amino-[1,1'-biphenyl]-4-yl)-3-(3-(cyclopentyloxy)-4-methoxyphenyl) acrylamide ***(24)***

Yellow solid (yield: 47 %). ^{1}H NMR (400 MHz, Chloroform-*d*) *δ* 10.08 (s, 1H), 7.81 – 7.60 (m, 2H), 7.59 – 7.46 (m, 3H), 7.41 – 7.28 (m, 2H), 7.18 (d, *J* = 7.2 Hz, 2H), 7.01 (d, *J* = 8.4 Hz, 1H), 6.77 – 6.56 (m, 3H), 4.85 (tt, *J* = 6.0, 2.7 Hz, 1H), 3.79 (s, 3H), 1.94 (dh, *J* = 11.1, 4.3, 3.7 Hz, 2H), 1.75 (tt, *J* = 8.4, 4.6 Hz, 4H), 1.60 (ddq, *J* = 11.7, 8.9, 5.7 Hz, 2H). ^{13}C NMR (100 MHz, Chloroform-*d*) *δ* 168.90, 156.44, 153.24, 152.39, 145.35, 142.54, 140.90, 132.72, 132.39, 131.97, 130.74, 126.79, 125.11, 124.71, 119.47, 118.37, 117.46, 84.81, 60.83, 37.52, 28.85. HRMS (ESI) *m/z* calcd for $C_{27}H_{28}N_2O_3$ $[M+H]^+$: 429.2100; Found: 429.2117.

(E)-3-(4-(cyclopentyloxy)-3-methoxyphenyl)-N-((1S,3S,5S,7S)-3,5-dimethyladamantan-1-yl) acrylamide ***(13)***

White solid (yield: 41 %). ^{1}H NMR (400 MHz, Chloroform-*d*) *δ* 7.47 (d, *J* = 15.4 Hz, 1H), 7.08 – 6.95 (m, 2H), 6.83 (d, *J* = 8.2 Hz, 1H), 6.19 (d, *J* = 15.4 Hz, 1H), 5.34 (s, 1H), 4.79 (tt, *J* = 6.4, 3.2 Hz, 1H), 3.85 (s, 3H), 2.16 (h, *J* = 3.2 Hz, 1H), 2.01 – 1.77 (m, 8H), 1.72 (s,

4H), 1.67 – 1.55 (m, 2H), 1.41 (dt, J = 12.3, 2.6 Hz, 2H), 1.35 – 1.27 (m, 2H), 1.26 – 1.11 (m, 2H), 0.86 (s, 6H). ^{13}C NMR (100 MHz, Chloroform-*d*) δ 165.34, 149.89, 140.21, 127.66, 121.83, 119.74, 114.14, 110.30, 80.39, 56.04, 53.73, 50.62, 47.70, 42.70, 40.31, 32.88, 32.43, 30.18, 30.10, 24.15. HRMS (ESI) *m/z* calcd for $C_{27}H_{37}NO_3$ $[M+H]^+$: 424.2773; Found: 424.2782.

*(E)-3-(3-(cyclopentyloxy)-4-methoxyphenyl)-N-((1S,3S,5S,7S)-3,5-dimethyladamantan-1-yl) acrylamide (**25**)*

White solid (yield: 44 %). ^{1}H NMR (400 MHz, Chloroform-*d*) δ 7.47 (d, J = 15.4 Hz, 1H), 7.10 – 6.96 (m, 2H), 6.82 (d, J = 8.3 Hz, 1H), 6.18 (d, J = 15.4 Hz, 1H), 5.37 (s, 1H), 4.78 (tt, J = 6.3, 3.2 Hz, 1H), 3.86 (s, 3H), 2.17 (hept, J = 3.2 Hz, 1H), 1.99 – 1.80 (m, 8H), 1.72 (t, J = 2.0 Hz, 4H), 1.67 – 1.55 (m, 2H), 1.41 (dt, J = 12.3, 2.7 Hz, 2H), 1.35 – 1.27 (m, 2H), 1.24 – 1.12 (m, 2H), 0.86 (s, 6H). ^{13}C NMR (100 MHz, Chloroform-*d*) δ 165.36, 151.42, 147.70, 140.28, 127.87, 121.55, 119.79, 113.48, 111.63, 80.50, 56.02, 53.76, 50.62, 47.70, 42.70, 40.29, 32.84, 32.43, 30.18, 30.10, 24.11. HRMS (ESI) *m/z* calcd for $C_{27}H_{37}NO_3$ $[M+H]^+$: 424.2773; Found: 424.2779.

(E)-3-(4-(cyclopentyloxy)-3-methoxyphenyl)-N-(4-(4-methylpiperazin-1-yl)phenyl) acrylamide (**14**)

Yellow solid (yield: 55.13 %). ^{1}H NMR (400 MHz, $CDCl_3$) δ 7.67 (d, J = 15.4 Hz, 1H), 7.52 (s, 3H), 7.12 – 6.97 (m, 2H), 6.88 (dd, J_1 = 25.6, J_2 = 8.5 Hz, 3H), 6.43 (d, J = 15.4 Hz, 1H), 4.81 (s, 1H), 3.86 (s, 3H), 3.19 (s, 4H), 2.71 – 2.46 (m, 4H), 2.37 (s, 3H), 1.90 (dd, J_1 = 30.0, J_2 = 10.4 Hz, 6H), 1.63 (s, 2H). ^{13}C NMR (100 MHz, Chloroform-*d*) δ 164.36,

151.56, 148.11, 147.69, 141.48, 130.89, 127.79, 121.56, 121.27, 119.07, 116.52, 113.79, 111.73, 80.55, 77.40, 77.09, 76.77, 55.95, 55.06, 49.38, 46.09, 32.79, 29.69, 24.06. HRMS (ESI) *m/z* calcd for $C_{26}H_{33}N_3O_3$ $[M+H]^+$: 436.2601; Found: 436.2595.

(E)-3-(3-(cyclopentyloxy)-4-methoxyphenyl)-N-(4-(4-methylpiperazin-1-yl)phenyl) acrylamide (**26**)

Yellow solid (yield: 58.96 %). ^{1}H NMR (400 MHz, $CDCl_3$) δ 7.65 (d, J = 15.4 Hz, 1H), 7.50 (d, J = 6.2 Hz, 2H), 7.31 (s, 1H), 7.12 – 7.02 (m, 2H), 6.91 (d, J = 8.9 Hz, 2H), 6.84 (d, J = 8.2 Hz, 1H), 6.38 (d, J = 15.4 Hz, 1H), 4.78 (s, 1H), 3.87 (s, 3H), 3.18 (d, J = 4.5 Hz, 4H), 2.63 – 2.51 (m, 4H), 2.35 (s, 3H), 1.87 (dd, J_1 = 15.3, J_2 = 10.9 Hz, 6H), 1.68 (s, 2H). ^{13}C NMR (100 MHz, Chloroform-*d)* δ 164.24, 149.88, 149.53, 148.14, 141.64, 130.83, 127.45, 122.00, 121.25, 118.74, 116.61, 114.11, 110.59, 80.44, 77.38, 77.06, 76.74, 55.99, 55.04, 49.40, 46.08, 32.87, 29.71, 24.14.HRMS (ESI) *m/z* calcd for $C_{26}H_{33}N_3O_3$ $[M+H]^+$: 436.2609; Found: 436.2595.

2 Reagents materials

Dulbecco's modified Eagle's medium (DMEM), and fetal bovine serum (FBS) were purchased from Gibco (Grand Island, NY, USA). Dimethyl sulfoxide (DMSO), Trypsin, thiazolyl blue tetrazolium bromide (MTT), lipopolysaccharide (LPS) and anti-GAPDH antibody were purchased from Sigma Aldrich (St. Louis, MO, USA). Tested compounds were dissolved in DMSO and stored at -20ºC. Anti-β-Actin antibody was purchased from Thermo Fisher. Anti-CREB phosphorylated and anti- NF-κB p65 were from Cell Signaling

Technology. Anti-Lamin B, anti-HO-1, anti-MMP2 and anti-MMP9 antibodies were obtained from Abcam. Anti-BDNF antibody was obtained Santa cruz.

2.1 Cell cultures

HT22 cell was an immortalized cell line from mouse hippocampus, which was a gift from Prof. Jun Liu, Sun Yat-Sen Memorial Hospital, Sun Yat-Sen University, China. BV2 cell was a murine microglial cell line, obtained from China Center for Type Culture Collection, catalog number: GDC311. Cells were cultured in DMEM s containing 10 % FBS and incubated at 37ºC under 5% CO_2.

2.2 MTT assay and LDH assay

Cell toxicity and viability were estimated by MTT assay and LDH assay. The release of LDH in the culture medium was estimated through an LDH Release Assay Kit (Beyotime, China). HT22 cells were cultured in 96-well plates at the concentration of 1×10^5/mL and exposed to compound **5** (3, 10, 30, 100 and 300 μM) for 24 h. 20 μL supernatant per well was added into a 96-well microplate to estimate LDH levels according to the manufacturer's instructions. The absorbance was measured through a multi-mode reader (Bio-Tek, USA) at 540 nm.

For the MTT assay, HT22 cells were cultured in 96-well plates at the concentration of 1×10^5/mL. Cells were exposed to compounds (1, 3, 10 and 100 μM) for 24 h. Or cells were treated with compounds (1, 3,10 μM) for 30 min and then exposed to glutamate (3 mM) for another 24 h. 10 μL MTT (5 mg/ml) was added and incubated for 2 h at 37 °C. MTT reagent

was removed out and then replaced with DMSO (100 μL). After shaking at room temperature for 10 min, the absorbance was measured through a multi-mode reader at 570 nm. Results were expressed as the percentage of untreated cells. Each concentration had at least three replicates. For MTT and LDH assays, all data were represented as mean ± SEM from three independent experiments.

2.3 Measurement of nitric oxide (NO)

NO generation in the medium was determined in the culture supernatant using Griess reagents (Beyotime, S0021). BV2 cells were grown at 4×10^4 cells per well in 96-well plates and then incubated for 24 h. The cells were pretreated with or without compound **5** at 1, 3, 10 μM for 2 h, then add LPS (1 μg/mL) in the wells for 24 h. To evaluate the NO levels, take out the Griess reagent Ⅰ and Ⅱ to return to room temperature. Dilute the standard sample with the solution of 1-100 μM using culture medium. Add standard diluent and the supernatant 50 μL respectively into 96 well plate. Add equal volume of Griess reagents Ⅰ and Ⅱ (50 μL) were mixed at room temperature. Incubate the mixture at room temperature for 15 min. Then the absorbance of the mixture was measured in a microplate absorbance reader at 540 nm. Each concentration had four replicates in three independent experiments.

2.4 Extraction of cytoplasmic and nuclear proteins

At 2 h after drug treatment, the BV2 cells were harvested and washed 3 times with cold phosphate-buffered saline (PBS). The cytoplasmic and nuclear protein fractions were extracted using Active Motif nuclear extraction kits (40010) according to the manufacturer's protocol. Add cold phosphatase inhibitor solution. Cells were collected to a new EP tube at

12000 g, 10 min, 4℃. Discard the supernate and resuspend the pellet with hypotonic buffer for 15 min. Centrifuge the solution at 14,000 g 4℃ for 3 min. Keep the supernate for cytoplasmic proteins. Use complete lysis buffer to resuspend the pellet for 30 min. Centrifuge the solution for 14,000 g 4℃ for 10 min. Keep the liquid for nuclear proteins. Cytoplasmic and nuclear protein extracts were used for Western blot analysis.

2.5 Western blotting

HT22 or BV2 cells was plated at a density of 1×10^6/mL in 6-well plate and pretreated with compounds and then stimulated with LPS (1 μg/mL) for 24 h. Then the cells were lysed with lysis buffer on ice. Collect the lysates centrifuging at 12,000 rpm for 15 min at 4°C and the concentrations of protein were quantified with BCA assay. For the animal experiment, the hippocampus and cortex tissues were flash frozen and stored at -80°C until homogenization. The tissues were homogenized with lysis buffer containing protease and phosphatase inhibitor. Then the homogenates were centrifuged at 12,000 rpm for 15 min at 4°C and the concentrations of protein were quantified with BCA assay. Protein samples were separated by using 10% SDS-PAGE and then transferred to a polyvinylidene fluoride membrane and incubated with 5% BSA at room temperature for 2 h. Then the membranes were incubated with the primary antibodies overnight at 4°C. Then the membranes were washed with a tris buffered saline/t buffer for 30 min and then incubated with secondary antibodies at room temperature for 1.5 h. The protein bands were visualized by using an ECL Prime kit (Millipore, USA). Three independent experiments were implemented.

2.6 Immunofluorescence

Cells were seeded and cultured on coverslips in 24 well plates. When the cells came to 60 % -70 % confluence, take various drug administration. After treatment, discard the supernate and wash with cold PBS. Then fixed with 4% paraformaldehyde for 20 min at room temperature. After washing three times with ice-cold PBS, cells were merged with 0.1% TritonX-100 for 10 min, and then incubated with 10% goat serum at room temperature for 1 h. Cells were incubated with primary antibodies against p-CREB (1:200), NF-*κ*B (1:250) at 4 °C overnight. After washing three times with ice-cold PBS, cells were incubated with goat-anti-rabbit secondary antibodies conjugated to Alexa Fluor 488 (Invitrogen, Carlsbad, CA) for 60 min at room temperature in the dark. The nuclei were incubated with DAPI (Beyotime, China, catalog, C1002, 5 mg/ml in PBS) in the dark for 8 min at room temperature. Take out the coverslips and transfer them on slides with anti-fluorescence quenching agent. Immunofluorescent images were acquired through a confocal microscope (Olympus FV3000, Japan).

2.7 Animals

All the animal experiments were approved by the Ethics Committee on the Care and Use of Laboratory Animals of Sun Yat-sen University (Guangzhou, China). KunMing mice (20 - 25 g, 8 w, male) were purchased from Sun Yat-sen University Animal Center. All mice were housed in a temperature- (20 ± 2 °C) and humidity-controlled room with 12 h dark/light cycle with food and water available ad libitum.

2.8 Animal experimental protocol

All experiments were approved by the local ethics committee. According to the model of cortical injury, the modified rubber bullet impact model was built in our laboratory. The rubber bullet was shot by an air gun to damage the unilateral cortex of mice. The modeling procedures were as follows: firstly, the mice were anesthetics by intraperitoneal injection of 1% pentobarbital sodium (50 mg/kg). Then, the scalpel was used to cut into the scalp of the mouse, and the skull was exposed. A marker was used to mark the striking area on the right hemisphere (3 mm lateral and 1 mm posterior to the bregma). Then, the air gun is loaded with rubber bullets and loaded. The iron ring of the muzzle is aimed at the hit area, and 2 shots are fired. Stitch up the wound quickly; Finally, the mice were put back into their cages. Mice were randomly divided into four groups designated as follows: the sham group (*n*= 10), the modeling group (*n*= 10), the TBI + compound **5** (5 mg/kg, HPLC, 99.14%) group (*n*= 10), the TBI + compound **5** (10 mg/kg) group (*n*= 10). Compound **5** was administered by gavage in two divided doses, and was administered at 0 h and 6 h after awaking. Mice were sacrificed at 48 h after modeling.

2.9 Measurement of BBB Permeability by Evans Blue (EB)

Colorimetry detection of extravasated EB dye was used to evaluate BBB disruption of the mice after TBI quantitatively. Briefly, one hour before sacrifice, EB dye (Sigma, freshly dissolved in sterile saline, 2% *w/v* in PBS) was injected into the tail vein (4 mL/kg). After about one hour, mice were deeply anesthetized with 1% pentobarbital sodium (50 mg/kg, i.p.). Then rapidly perfuse from the left ventricle to the right atrium using normal saline until the effluent clarifies. Brains were quickly removed. Afterwards wash out the blood on the

surface with 0.9 % NaCl. Put the tissues in formamid (10 mL/g) for homogenization and incubate the brains for 24 h at 60℃ water bathe. Then centrifuge the homogenate at 4,000 rpm for 20 mins at 4 °C. Fluorescence values of the supernatant were analyzed by a fluorescence spectrophotometer at the wavelength of 632 nm. The contents of EB dye were quantified from a linear standard curve.

2.10 Statistical analysis

The data were presented as means ± SD for at least 3 experiments. Statistical differences between the groups were examined using one-way analysis of variance (ANOVA), followed by a Tukey-Kramer test. The significance of the results was determined at $P<0.05$.

Associated contents

Supporting Information

^{1}H and ^{13}C NMR data of compounds 3-26. HPLC data of compounds 5, 6, 8, 12, 13, 15, 18, 24. PDE4B2 and PDE4D7 kinase activity assay of compound 5.

Author information

Corresponding Author

*E-mail: pirb@mail.sysu.edu.cn

ORCID

Rongbiao Pi: 0000-0001-8150-9164

Author Contributions

Rongbiao Pi and Junfeng Lu designed and conducted the experiments and wrote the manuscript. In vitro assays were carried out by Junfeng Lu. In vivo studies and data analysis were carried out by Chen Chen and Junfeng Lu. Xiaobing Deng performed molecular docking. Chen Chen and Zeyu Zhu synthesized and characterized the compounds. Xixin He and Jinhao Liang helped to conduct the experiments. Marvin SH Mak, Swetha K. Maddili, Karl M Tism, Yifan Han provided insight into interpretation of the results and revised the manuscript.

Present Address Department of Pharmacology & Toxicology, School of Pharmaceutical Sciences, Sun Yat-Sen University 132#, Waihuan Dong Road, High Education Mega Center, Guangzhou

Acknowledgements

This study was supported by Grants from National Natural Scientific Foundation Committee (№81671264), Guangzhou Scientific Foundation Committee (№201704020222 to Z Zuo and R Pi, № 201807010094 to X Li and R PI) and the Hong Kong Polytechnic University (G-YBGQ, G-YZ95, G-SB81), ITSP-Guangdong Hong Kong Technology Cooperation Funding Scheme (GHP/012/16GD), Shenzhen Basic Research Program (JCYJ20160331141459373) to YF. Han.

Notes

The authors declared there is no interest conflicts.

Abbreviations

TBI, Traumatic brain injury; HO-1, heme oxygenase-1; P-CREB the phosphorylated cAMP response elements binding protein; CNS, central nervous system; AD, Alzheimer's disease; Neurodegenerative diseases, NNDs; PDE4, phosphodiesterase-4; BBB, blood-brain barrier; LTP, long-term potentiation; Nrf2, nuclear factor-related factor 2; HO, heme oxygenase; BDNF, brain-derived neurotrophic factor; CREB, Cyclic AMP response protein element binding protein; PD, Parkinson's disease; NO, nitric oxide; ROS, reactive oxygen species; TNF-α, tumor necrosis factor; IL-1β, interleukin; LPS, lipopolysaccharide; clog P, octanol–water partitioning coefficient; MW, molecular weight; LD_{50}, the median lethal dose; PROTAC, PROteolysis Targeting Chimeras; MMP, Matrix metalloproteinase; TLC, Thin-layer chromatography; NMR, nuclear magnetic resonance; HRMS, High-resolution mass spectrometric data; DMEM, Dulbecco's modified Eagle's medium; FBS, fetal bovine serum; DMSO, Dimethyl sulfoxide; MTT, thiazolyl blue tetrazolium bromide; LDH, lactate dehydrogenase; PBS, phosphate-buffered saline;

References

(1). Maas, A. I. R., Menon, D. K., Adelson, P. D., Andelic, N., Bell, M. J., Belli, A., Bragge, P., Brazinova, A., Buerki, A., Chesnut, R. M., Citerio, G., Coburn, M., Cooper, D. J., Crowder, A. T., Czeiter, E., Czosnyka, M., Diaz-Arrastia, R., Dreier, J. P., Duhaime, A. C., Ercole, A., van Essen, T. A., Feigin, V. L., Gao, G. Y., Giacino, J., Gonzalez-Lara, L. E., Gruen, R. L., Gupta, D., Hartings, J. A., Hill, S., Jiang, J. Y., Ketharanathan, N., Kompanje, E. J. O., Lanyon, L., Laureys, S., Lecky, F., Levin, H., Lingsma, H. F., Maegele, M., Majdan, M., Manley, G., Marsteller, J., Mascia, L., McFadyen, C., Mondello, S., Newcombe, V., Palotie, A., Parizel, P. M., Peul, W., Piercy, J., Polinder, S., Puybasset, L., Rasmussen, T. E., Rossaint, R., Smielewski, P., Soderberg, J., Stanworth, S. J., Stein, M. B., von Steinbuechel, N., Stewart, W., Steyerberg, E. W., Stocchetti, N., Synnot, A., Ao, B. T., Tenovuo, O., Theadom, A., Tibboel, D., Videtta, W., Wang, K. K. W., Williams, W. H., Wilson, L., Yaffe, K. InTBIR Participants and Investigators, (2017) Traumatic brain injury: integrated approaches to improve prevention, clinical care, and research. *Lancet Neurol.* 16, 987-1048.

(2). Jiang, J. Y., Gao, G. Y., Feng, J. F., Mao, Q., Chen, L. G., Yang, X. F., Liu, J. F., Wang, Y. H., Qiu, B. H., Huang, X. J., (2019) Traumatic brain injury in China. *Lancet Neurol.* 18, 286-295.

(3). Ladak, A. A., Enam, S. A., Ibrahim, M. T., (2019) A Review of the Molecular Mechanisms of Traumatic Brain Injury. *World Neurosurg.* 131, 126-132.

(4). Stoica B. A, Faden A. I., (2010) Cell death mechanisms and modulation in traumatic brain injury. *Neurotherapeutics.* 7, 3-12.

(5). Ray, SK., Dixon, CE., Banik, NL., (2002) Molecular mechanisms in the pathogenesis of traumatic brain injury. *Histol Histopathol.* 17, 1137-1152.

(6). Marshall, T. M., Dardia, G. P., Colvin, K. L., Nevin, R., Macrellis, J., (2019) Neurotoxicity Associated with Traumatic Brain Injury, Blast, Chemical, Heavy Metal and Quinoline Drug Exposure. *Altern. Ther. Health Med.* 25, 28-34.

(7). Reis, C., Wang, Y. C., Akyol, O., Ho, W. M., Ii, Applegate, R., Stier, G., Martin, R., Zhang, J. H., (2015) What's New in Traumatic Brain Injury: Update on Tracking, Monitoring and Treatment. *Int. J. Mol. Sci.* 16, 11903-11965.

(8). Bawa, P., Pradeep, P., Kumar, P., Choonara, Y. E., Modi, G., Pillay, V., (2016) Multi-target therapeutics for neuropsychiatric and neurodegenerative disorders. *Drug Discov. Today* 21, 1886-1914.

(9). Somayaji, M. R., Przekwas, A. J, Gupta, R. K., (2018) Combination Therapy for Multi-Target Manipulation of Secondary Brain Injury Mechanisms. *Curr Neuropharmacol.,* 16, 484–504.

(10). Wilson, N. M., Titus, D. J., Oliva, A. A., Furones, C., Atkins, C. M., (2016) Traumatic Brain Injury Upregulates Phosphodiesterase Expression in the Hippocampus. *Front Syst Neurosci*. 10, 5.

(11). Titus, D. J., Sakurai, A., Kang, Y., Furones, C., Jergova, S., Santos, R., Sick, T. J., Atkins, C. M., (2013) Phosphodiesterase inhibition rescues chronic cognitive deficits induced by traumatic brain injury. *J Neurosci.* 33, 5216-5226.

(12). Pettipher, E. R., Labasi, J. M., Salter, E. D., Stam, E. J., Cheng, J. B., Griffiths, R. J., (1996) Regulation of tumour necrosis factor production by adrenal hormones in vivo: insights into the antiinflammatory activity of rolipram. *Br. J. Pharmacol.* 117, 1530-1534.

(13). Bruno, O., Romussi, A., Spallarossa, A., Brullo, C., Schenone, S., Bondavalli, F., Vanthuyne, N., Roussel, C., (2009) New selective phosphodiesterase 4D inhibitors differently acting on long, short, and supershort isoforms. *J. Med. Chem.* 52, 6546-6557.

(14). Atkins, C. M., Cepero, M. L., Kang, Y., Liebl, D. J., Dietrich, W. D., (2013) Effects of early rolipram treatment on histopathological outcome after controlled cortical impact injury in mice. *Neurosci. Lett.* 532, 1-6.

(15). Burgin, A. B., Magnusson, O. T., Singh, J., Witte, P., Staker, B. L., Bjornsson, J. M., Thorsteinsdottir, M., Hrafnsdottir, S., Hagen, T., Kiselyov, A. S., Stewart, L. J., Gurney, M. E., (2010) Design of

phosphodiesterase 4D (PDE4D) allosteric modulators for enhancing cognition with improved safety. *Nat. Biotechnol.* 28, 63-70.

(16). Brullo, C., Ricciarelli, R., Prickaerts, J., Arancio, O., Massa, M., Rotolo, C., Romussi, A., Rebosio, C., Marengo, B., Pronzato, M. A., van Hagen, B., van Goethem, N. P., D'Ursi, P., Orro, A., Milanesi, L., Guariento, S., Cichero, E., Fossa, P., Fedele, E., Bruno, O., (2016) New insights into selective PDE4D inhibitors: 3-(Cyclopentyloxy)-4-methoxybenzaldehyde O-(2-(2,6-dimethylmorpholino)-2-oxoethyl) oxime (GEBR-7b) structural development and promising activities to restore memory impairment. Eur. *J. Med. Chem.* 124, 82-102.

(17). National Institute of Neurological Disorders and Stroke (NINDS), (2001) Rolipram to Treat Multiple Sclerosis. https://clinicaltrials.gov/ct2/show/NCT00011375

(18). Glaxo, Smith K., (2012) Healthy Volunteer Positron Emission Tomography (PET) Brain Occupancy Study of a Phosphodiesterase-4 (PDE4) Inhibitor in Huntington's Disease. https://clinicaltrials.gov/ct2/show/NCT01602900

(19). Hu, J. H., Pan, T. T., An, B. J., Li, Z. C. X., Li, X. S., Huang, L., (2019) Synthesis and evaluation of clioquinol-rolipram/roflumilast hybrids as multitarget-directed ligands for the treatment of Alzheimer's disease. *Eur J Med Chem.* 163, 512-526.

(20). Brullo, C., Massa, M., Villa, C., Ricciarelli, R., Rivera, D., Pronzato, M. A., Fedele, E., Barocelli, E., Bertoni, S., Flammini, L., Bruno, O., (2015) Synthesis, biological activities and pharmacokinetic properties of new fluorinated derivatives of selective PDE4D inhibitors. *Bioorg Med Chem.* 23, 3426-3435.

(21). Zhuo, Y., Zhuo, J., (2019) Tranilast Treatment Attenuates Cerebral Ischemia-Reperfusion Injury in Rats Through the Inhibition of Inflammatory Responses Mediated by NF-kappaB and PPARs. *Clin. Transl. Sci.* 12, 196-202.

(22). Huang, Y., Jiang, H., Chen, Y., Wang, X., Yang, Y. Q., Tao, J. H., Deng, X. M., Liang, G. L., Zhang, H. F., Jiang, W., Zhou, R. B., (2018) Tranilast directly targets NLRP3 to treat inflammasome-driven diseases. *EMBO Mol. Med*. 10, 1-15.

(23). Darakhshan, S., Pour, A. B., (2015) Tranilast: a review of its therapeutic applications. *Pharmacol. Res.* 91, 15-28.

(24). Rogosnitzky, M., Danks, R., Kardash, E., (2012) Therapeutic potential of tranilast, an anti-allergy drug, in proliferative disorders. *Anticancer Res.* 32, 2471-2478.

(25). Sun, X. M., Suzuki, K., Nagata, M., Kawauchi, Y., Yano, M., Ohkoshi, S., Matsuda, Y., Kawachi, H., Watanabe, K., Asakura, H., Aoyagi, Y., (2010) Rectal administration of tranilast ameliorated acute colitis in mice through increased expression of heme oxygenase-1. *Pathol Int.* 60, 93-101.

(26). Pae, H. O., Jeong, S. O., Koo, B. S., Ha, H. Y., Lee, K. M., Chung, H. T., (2008) Tranilast, an orally active anti-allergic drug, up-regulates the anti-inflammatory heme oxygenase-1 expression but down-regulates the pro-inflammatory cyclooxygenase-2 and inducible nitric oxide synthase expression in RAW264.7 macrophages. *Biochem Biophys Res Commun.* 371, 361-365.

(27). Miyachi, Y., Imamura, S., Niwa, Y., (1987) The effect of tranilast of the generation of reactive oxygen species. *J Pharmacobio dyn.* 10, 255-259.

(28). Yang, W., Sabi-Mouka, E. M. B., Wang, L., Shu, C., Wang, Y., Ding, J. F., Ding, L., (2018) Determination of tranilast in bio-samples by LC-MS/MS: Application to a pharmacokinetic and brain tissue distribution study in rats. *J Pharm Biomed Anal.* 147, 479-484.

(29). Makhouri, F. R., Ghasemi, J. B., (2018) In Silico Studies in Drug Research Against Neurodegenerative Diseases. *Curr. Neuropharmacol.* 16, 664-725.

(30). Titus, D. J., Wilson, N. M., Alcazar, O., Calixte, D. A., Dietrich, W. D., Gurney, M. E.; Atkins, C. M., (2018) A negative allosteric modulator of PDE4D enhances learning after traumatic brain injury. *Neurobiol. Learn Mem.* 148, 38-49.

(31). Giudice, A., Arra, C., Turco, M. C., (2010) Review of molecular mechanisms involved in the activation of the Nrf2-ARE signaling pathway by chemopreventive agents. *Methods in Molecular Biology* 647, 37-74.

(32). Zhang, D. D., Hannink, M., (2003) Distinct cysteine residues in Keap1 are required for Keap1-dependent ubiquitination of Nrf2 and for stabilization of Nrf2 by chemopreventive agents and oxidative stress. *Mol. Cell Biol.* 23, 8137-8151.

(33). Liu, L., Locascio, L. M., Dore, S., (2019) Critical Role of Nrf2 in Experimental Ischemic Stroke. *Front Pharmacol.* 10, 153, 1-31.

(34). Bhardwaj, M., Deshmukh, R., Kaundal, M., Reddy, B. V. K., (2016) Pharmacological induction of hemeoxygenase-1 activity attenuates intracerebroventricular streptozotocin induced neurocognitive deficit and oxidative stress in rats. *Eur. J. Pharmacol.* 772, 43-50.

(35). Ko, H. R., Ahn, S. Y., Chang, Y. S., Hwang, I., Yun, T., Sung, D. K., Sung, S. I., Park, W. S., Ahn, J. Y., (2018) Human UCB-MSCs treatment upon intraventricular hemorrhage contributes to attenuate hippocampal neuron loss and circuit damage through BDNF-CREB signaling. *Stem Cell Res. Ther.* 9, 326-341.

(36). Nagahara, A. H., Tuszynski, M. H., (2011) Potential therapeutic uses of BDNF in neurological and psychiatric disorders. *Nat. Rev. Drug Discov.* 10, 209-219.

(37). Chen, A.; Xiong, L. J., Tong, Y., Mao, M., (2013) The neuroprotective roles of BDNF in hypoxic

ischemic brain injury. *Biomed. Rep.* 1, 167-176.

(38). Zhang, L., Zhao, H. Y., Zhang, X. J., Chen, L Y., Zhao, X. M., Bai, X., Zhang, J., (2013) Nobiletin protects against cerebral ischemia via activating the p-Akt, p-CREB, BDNF and Bcl-2 pathway and ameliorating BBB permeability in rat. *Brain Res. Bull.* 96, 45-53.

(39). Blokland, A., Heckman, P., Vanmierlo, T., Schreiber, R., Paes, D., Prickaerts, J., (2019) Phosphodiesterase Type 4 Inhibition in CNS Diseases. *Trends Pharmacol Sci*. 40, 971-985.

(40) Huang, H., Hong Q., H., Tan, H. L., Xiao, C. R., Gao, Y., (2016) Ferulic acid prevents LPS-induced up-regulation of PDE4B and stimulates the cAMP/CREB signaling pathway in PC12 cells. *Acta Pharmacol Sin.* 37, 1543–1554.

(41) Sawamoto, A., Okuyama, S., Nakajima, M., Furukawa, Y., (2019) Citrus flavonoid 3,5,6,7,8,3',4'-heptamethoxyflavone induces BDNF via cAMP/ERK/CREB signaling and reduces phosphodiesterase activity in C6 cells. *Pharmacol Rep.* 71, 653-658.

(42). Jung, Y. J., Xu, W. P., Kim, H., Ha, N., Neckers, L. (2007) Curcumin-induced degradation of ErbB2: A role for the E3 ubiquitin ligase CHIP and the Michael reaction acceptor activity of curcumin. *Biochim Biophys Acta*. 1773, 383-390.

(43). Groppe, J. C., (2019) Induced degradation of protein kinases by bifunctional small molecules a next generation strategy. *Expert Opin Drug Discov*. 14, 1237-1253.

(44). Churcher, I., (2018) Protac-Induced Protein Degradation in Drug Discovery: Breaking the Rules or Just Making New Ones? *J Med Chem.* 61, 444-452.

(45). Wang, Y., Jiang, X. Y., Feng, F., Liu, W. Y., Sun, H. P., (2020) Degradation of proteins by PROTACs and other strategies. *Acta Pharm Sin B.* 10, 207-238.

(46). Zhao, J. Y., Bi, W., Xiao, S., Lan, X., Cheng, X. F., Zhang, J. W., Lu, D. X., Wei, W., Wang, Y. P., Li, H. M., Fu, Y. M., Zhu, L. H., (2019) Neuroinflammation induced by lipopolysaccharide causes cognitive impairment in mice. *Sci. Rep.* 5790, 1-12.

(47). Kim, S. M., Ha, J. S., Han, A. R., Cho, S. W., Yang, S. J., (2019) Effects of alpha-lipoic acid on LPS-induced neuroinflammation and NLRP3 inflammasome activation through the regulation of BV-2 microglial cells activation. *BMB Rep.* 52, 613-618.

(48). Kumar, A., Henry, R. J., Stoica, B. A., Loane, D. J., Abulwerdi, G., Bhat, S. A., Faden, A. I., (2019) Neutral Sphingomyelinase Inhibition Alleviates LPS-Induced Microglia Activation and Neuroinflammation after Experimental Traumatic Brain Injury. *J. Pharmacol. Exp. Ther.* 368, 338-352.

(49). Al Sharif, M., Alov, P., Vitcheva, V., Diukendjieva, A., Mori, M., Botta, B., Tsakovska, I., Pajeva, I., (2017) Natural modulators of nonalcoholic fatty liver disease: Mode of action analysis and in silico ADME-Tox prediction. *Toxicol. Appl. Pharmacol.* 337, 45-66.

(50). Daina, A., Michielin, O., Zoete, V., (2017) SwissADME: a free web tool to evaluate pharmacokinetics, drug-likeness and medicinal chemistry friendliness of small molecules. *Sci Rep.* 7, 42717.

(51). Lipinski, C. A., Lombardo, F., Dominy, B. W., Feeney, P. J., (2001) Experimental and computational approaches to estimate solubility and permeability in drug discovery and development settings. *Adv Drug Deliv Rev.* 46, 3-26.

(52). Tonelli, M., Cichero, E., Mahmoud, A. M., Rabbito, A., Tasso, B., Fossa, P., Ligresti, A., (2018) Exploring the effectiveness of novel benzimidazoles as CB2 ligands: synthesis, biological evaluation, molecular docking studies and ADMET prediction. *Medchemcomm.* 9, 2045-2054.

(53). Maurya, S. S., Bahuguna, A., Khan, S. I., Kumar, D., Kholiya, R., Rawat, D. S., (2019) N-Substituted aminoquinoline-pyrimidine hybrids: Synthesis, in vitro antimalarial activity evaluation and docking studies. *Eur. J. Med. Chem.* 162, 277-289.

(54). Kaur, P., Sharma, S., (2018) Recent Advances in Pathophysiology of Traumatic Brain Injury. *Curr. Neuropharmacol.* 16, 1224-1238.

(55). Kinder, H. A., Baker, E. W., Wang, S. L., Fleischer, C. C., Howerth, E. W., Duberstein, K. J., Mao, H., Platt, S. R., West, F. D., (2019) Traumatic Brain Injury Results in Dynamic Brain Structure Changes Leading to Acute and Chronic Motor Function Deficits in a Pediatric Piglet Model. *J. Neurotrauma* 6303, 1-42.

(56). Titus, D. J., Wilson, N. M., Freund, J. E., Carballosa, M. M., Sikah, K. E., Furones, C., Dietrich, W. D., Gurney, M. E., Atkins, C. M., (2016) Chronic Cognitive Dysfunction after Traumatic Brain Injury Is Improved with a Phosphodiesterase 4B Inhibitor. *J. Neurosci.* 36, 7095-7108.

(57). Tang, L., Huang, C., Zhong, J. H., He, J. P., Guo, J. Y., Liu, M. H., Xu, J. P., Wang, H. T., Zhou, Z. Z., (2019) Discovery of arylbenzylamines as PDE4 inhibitors with potential neuroprotective effect. *Eur. J. Med. Chem.* 168, 221-231.

(58). Finnie, J. W., Manavis, J., Summersides, G. E., Blumbergs, P. C., (2003) Brain damage in pigs produced by impact with a non-penetrating captive bolt pistol. *Aust. Vet. J.* 81, 153-155.

(59). Pun, P. B., Lu, J., Moochhala, S., (2009) Involvement of ROS in BBB dysfunction. *Free Radic Res.* 43, 348-364.

(60). Kozler, P., Pokorny, J. (2003) Altered blood-brain barrier permeability and its effect on the distribution of Evans blue and sodium fluorescein in the rat brain applied by intracarotid injection. *Physiol. Res.* 52, 607-614.

(61). Vajtr, D., Benada. O., Kukacka, J. Prusa, R., Houstava, L., Toupalik, P.; Kizek, R. (2009) Correlation of ultrastructural changes of endothelial cells and astrocytes occurring during blood brain barrier damage after traumatic brain injury with biochemical markers of BBB leakage and inflammatory response. *Physiol. Res.* 58, 263-268.

Graphic abstract

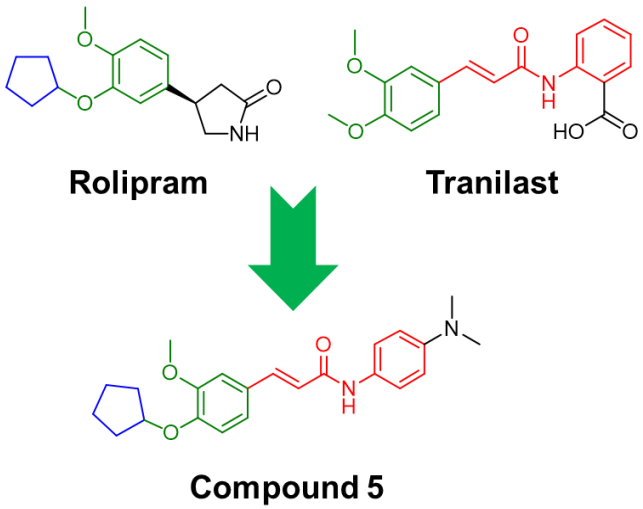

Nrf2/ HO-1 ↑

PDE4B ↓ p-CREB/ BDNF ↑

Nuclear translocation of NF-κB ↓ NO ↓

Bleeding area in brain tissue of TBI model ↓

Impaired blood-brain barrier ↓

In vitro

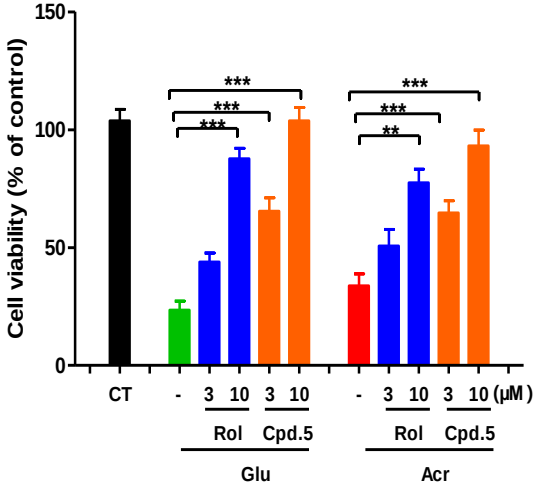

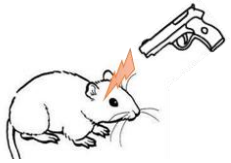

TBI model

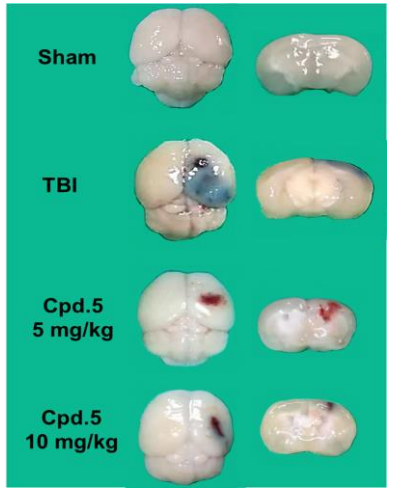

Figure 1

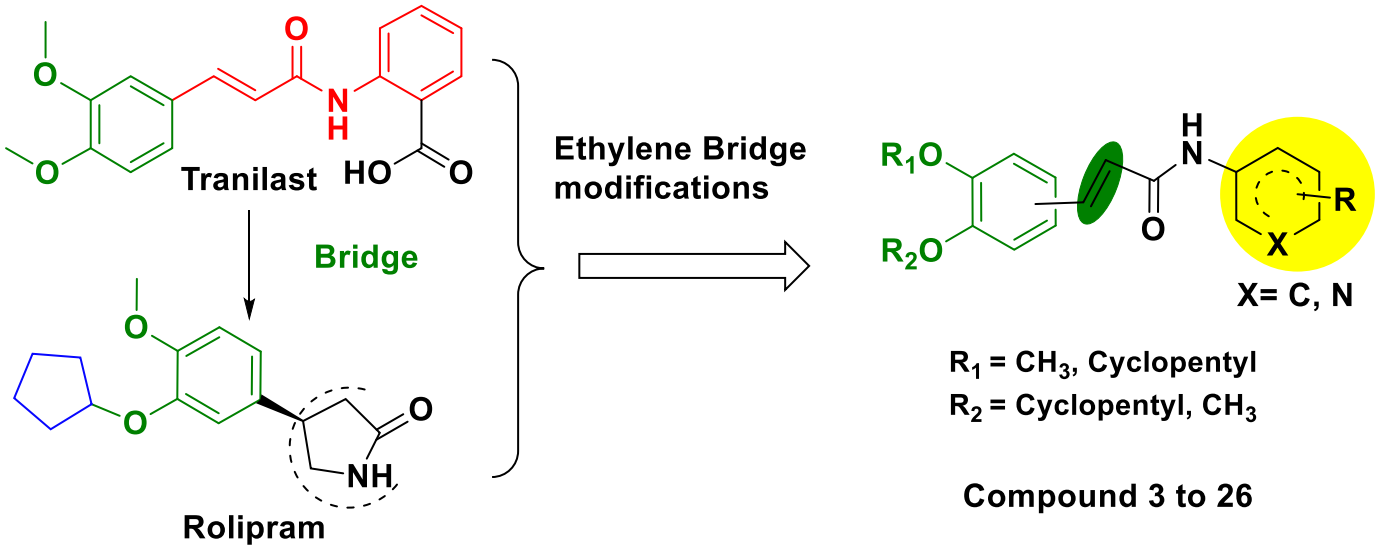
Tranilast
Bridge
Rolipram
Ethylene Bridge modifications
X= C, N
$R_1 = CH_3$, Cyclopentyl
R_2 = Cyclopentyl, CH_3
Compound 3 to 26

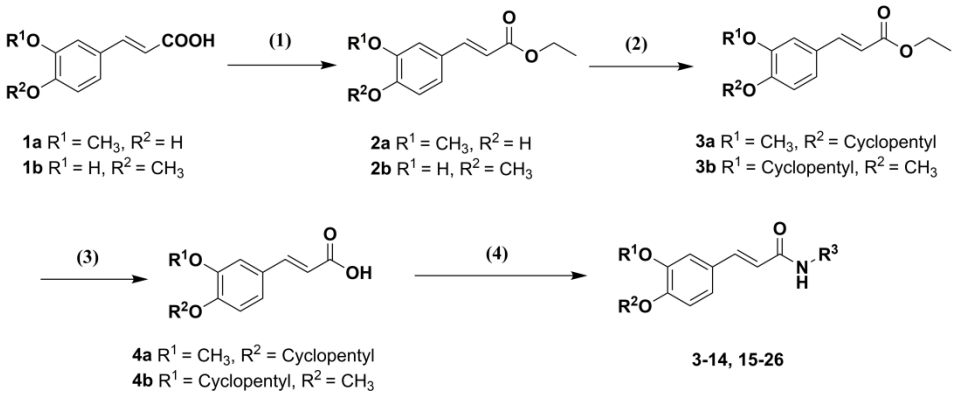

for 3-14: $R^1 = CH_3$, R^2 = Cyclopentyl **for 15-25:** R^1 = Cyclopentyl, $R^2 = CH_3$

R^3 = 2-OHPh, 3-CF_3Ph, 4-$N(CH_3)_2$Ph, Ph, 4-CF_3Ph, 4-NH_2Ph, 2-NH_2Ph, 2-NH_2,

4-FPh, 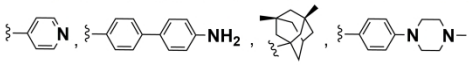

Reagents and conditions: (1) H_2SO_4 conc., ethanol, reflux; (2) Bromocyclopentane, K_2CO_3, DMF,65 ^oC; (3) 20% NaOH, THF, reflux; (4) RNH_2,EDCI, HOBt ,DCM, rt.

Synthesis of the target compounds 3-26.

196x132mm (600 x 600 DPI)

Figure 2

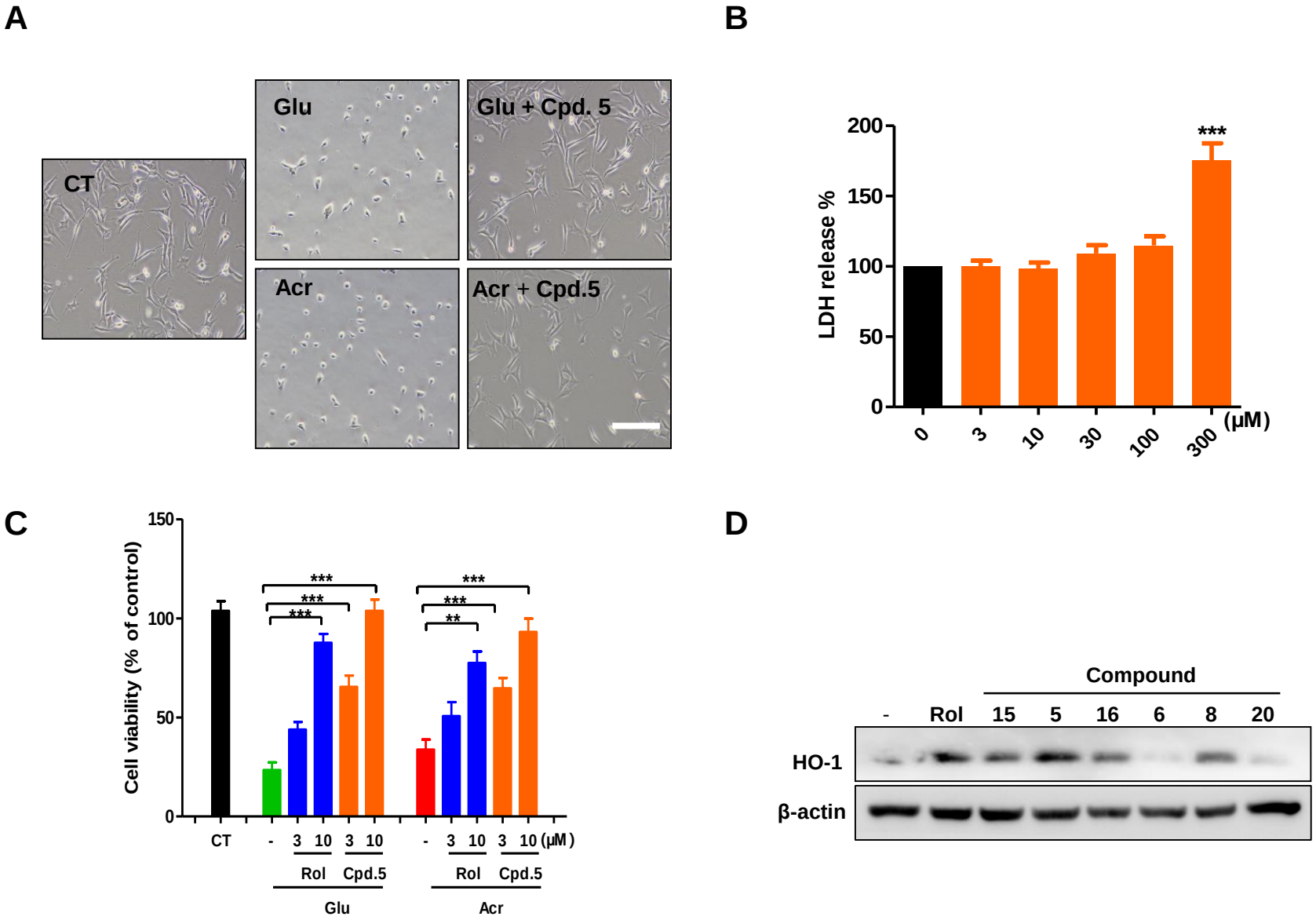
A
CT
Glu
Glu + Cpd. 5
Acr
Acr + Cpd.5
B
LDH release %
200
150
100
50
0
***
0
3
10
30
100
300
(μM)
C
Cell viability (% of control)
150
100
50
0
***
***
***
***
***
**
CT
-
3
10
3
10
-
3
10
3
10 (μM)
Rol
Cpd.5
Rol
Cpd.5
Glu
Acr
D
Compound
-
Rol
15
5
16
6
8
20
HO-1
β-actin

Figure 3

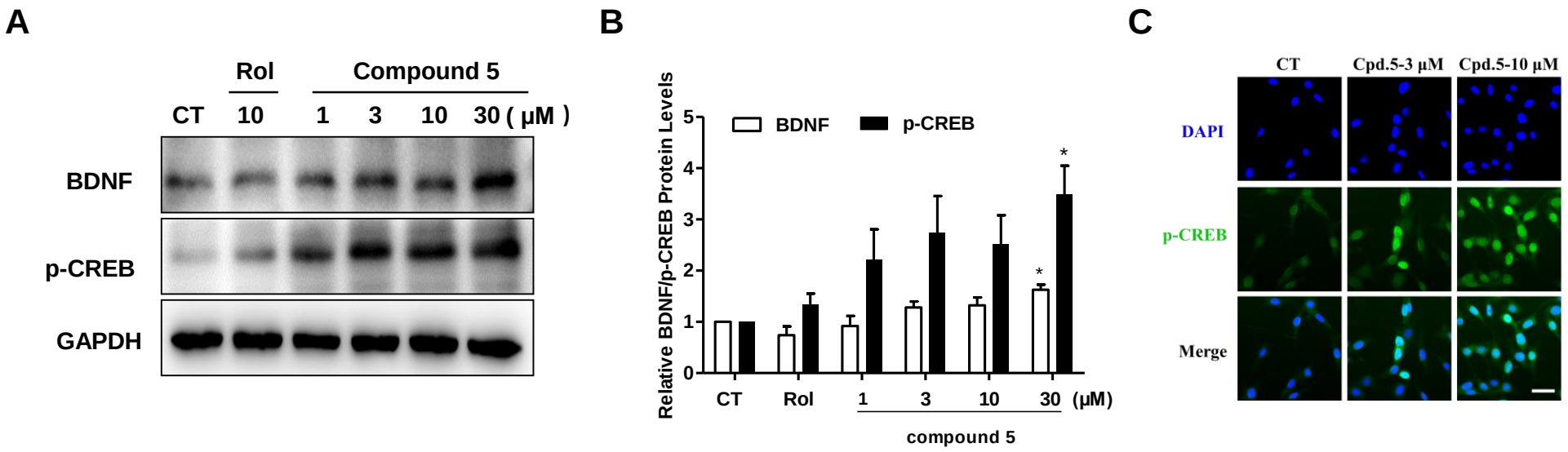
A
Rol
Compound 5
CT
10
1
3
10
30 (μM)
BDNF
p-CREB
GAPDH
B
Relative BDNF/p-CREB Protein Levels
BDNF
p-CREB
CT
Rol
1
3
10
30
(μM)
compound 5
C
CT
Cpd.5-3 μM
Cpd.5-10 μM
DAPI
p-CREB
Merge

Figure 4

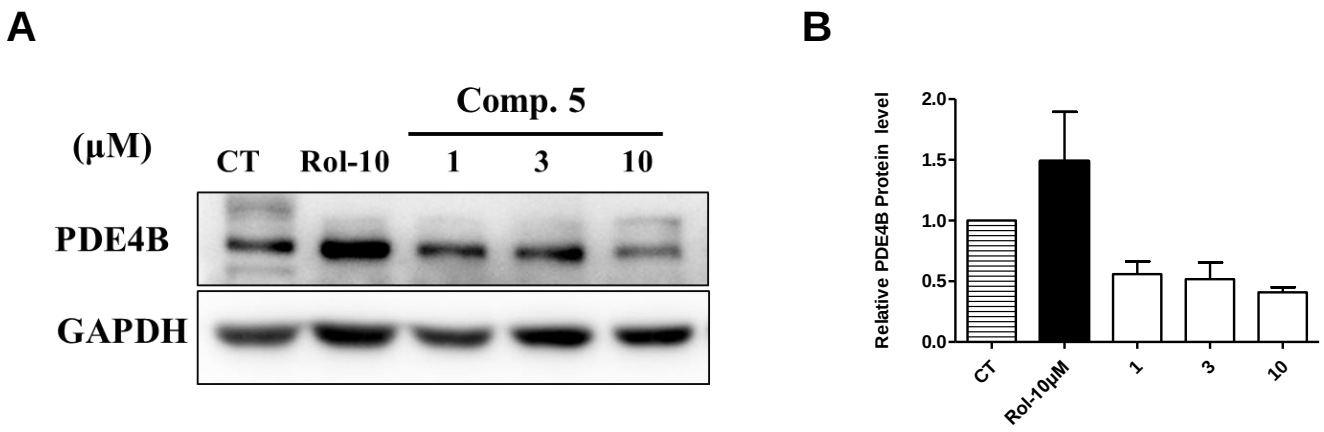
A
Comp. 5
(μM)
CT
Rol-10
1
3
10
PDE4B
GAPDH
B
Relative PDE4B Protein level
2.0
1.5
1.0
0.5
0.0
CT
Rol-10μM
1
3
10

Figure 5

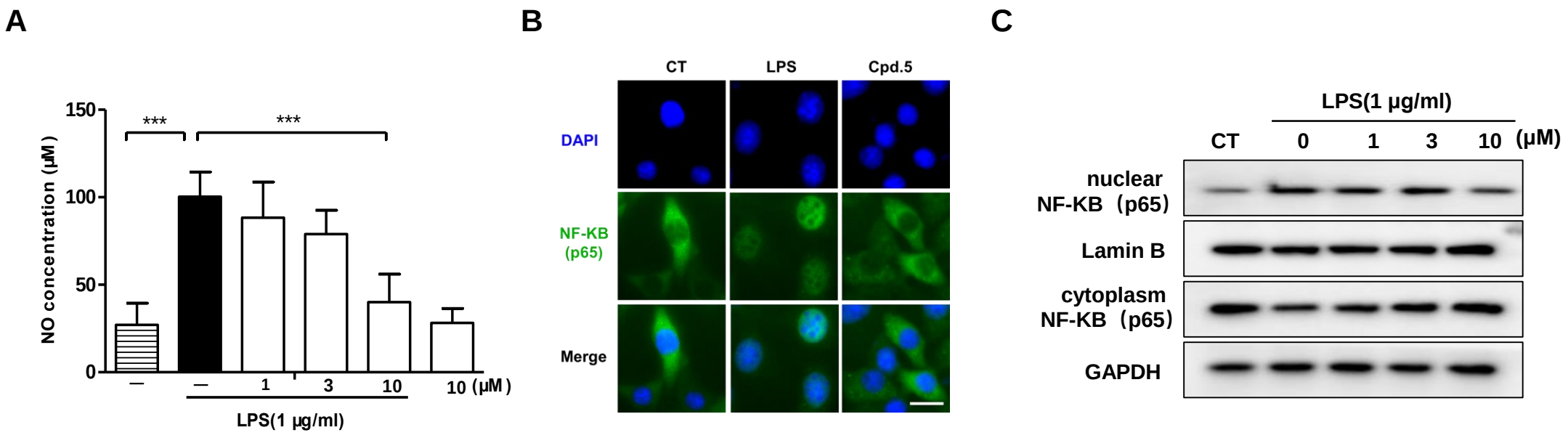
A
150
100
50
0
NO concentration (μM)
***
***
—
—
1
3
10
10 (μM)
LPS(1 μg/ml)
B
CT
LPS
Cpd.5
DAPI
NF-KB
(p65)
Merge
C
LPS(1 μg/ml)
CT
0
1
3
10
(μM)
nuclear
NF-KB (p65)
Lamin B
cytoplasm
NF-KB (p65)
GAPDH

Figure 6

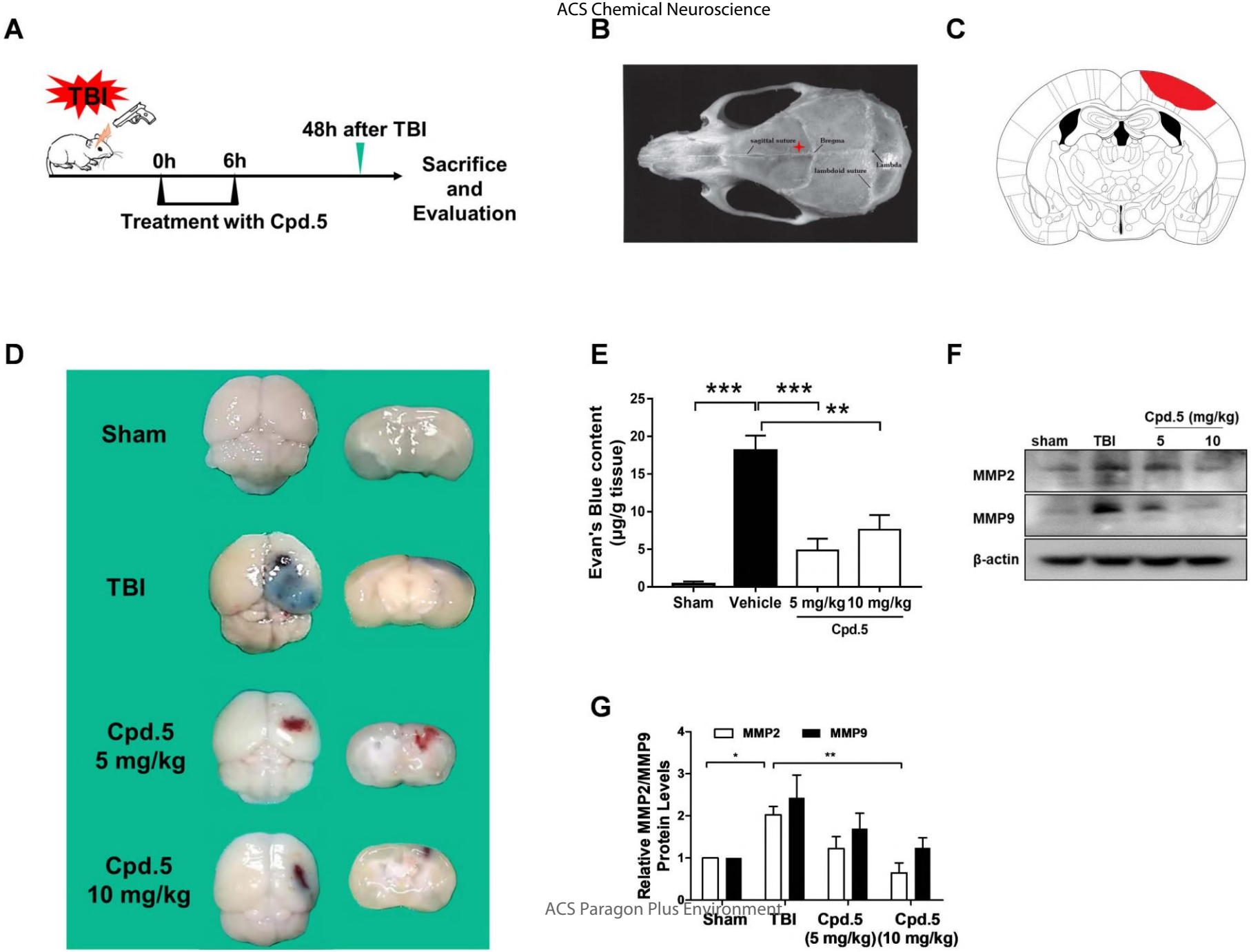
A
TBI
0h
6h
48h after TBI
Sacrifice and Evaluation
Treatment with Cpd.5
B
sagittal suture
Bregma
lambdoid suture
Lambda
C
D
Sham
TBI
Cpd.5 5 mg/kg
Cpd.5 10 mg/kg
E
Evan's Blue content (μg/g tissue)
***
***
**
Sham
Vehicle
5 mg/kg
10 mg/kg
Cpd.5
F
Cpd.5 (mg/kg)
sham
TBI
5
10
MMP2
MMP9
β-actin
G
MMP2
MMP9
Relative MMP2/MMP9 Protein Levels
Sham
TBI
Cpd.5 (5 mg/kg)
Cpd.5 (10 mg/kg)

Table 1. Neuroprotective and cytotoxic effects of compounds in HT22 cells.

Compd.	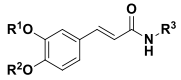			Cytotoxicity	Glutamate (3 mM)		Acrolein (20 μM)	
	R^1	R^2	R^3	100 μM	3 μM	10 μM	3 μM	10 μM
3	CH_3	C_5H_9	2-OHPh	54.1 ± 2.3	24.7 ± 0.8	46.0 ± 1.8	45.5 ± 0.5	49.3 ± 1.2
4	CH_3	C_5H_9	3-CF_3Ph	33.1 ± 1.3	24.8 ± 0.9	42.3 ± 0.6	42.0 ± 1.2	52.4 ± 0.7
5	CH_3	C_5H_9	4-$N(CH_3)_2$Ph	103.4 ± 1.3	75.8 ± 1.3	100.5 ± 1.2	72.8 ± 1.2	96.4 ± 1.4
6	CH_3	C_5H_9	Ph	69.7 ± 2.5	24.6 ± 0.4	56.5 ± 1.5	39.4 ± 1.1	52.6 ± 0.5
7	CH_3	C_5H_9	4-CF_3Ph	47.2 ± 1.8	28.0 ± 0.7	54.7 ± 0.6	37.7 ± 0.7	43.0 ± 0.6
8	CH_3	C_5H_9	4-NH_2Ph	83.5 ± 2.6	50.2 ± 1.4	81.3 ± 1.5	40.3 ± 0.6	79.2 ± 0.6
9	CH_3	C_5H_9	2-NH_2Ph	43.1 ± 1.3	27.7 ± 0.8	57.1 ± 1.5	38.9 ± 0.9	62.7 ± 1.2
10	CH_3	C_5H_9	2-NH_2,4-FPh	64.8 ± 1.9	24.0 ± 0.5	44.3 ± 1.4	37.1 ± 0.5	60.9 ± 1.0
11	CH_3	C_5H_9		23.7 ± 1.8	23.9 ± 0.9	51.7 ± 0.7	34.8 ± 0.7	43.6 ± 0.7
12	CH_3	C_5H_9	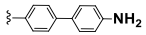	20.3 ± 1.8	25.0 ± 0.8	52.7 ± 0.7	36.0 ± 1.2	49.1 ± 1.4
13	CH_3	C_5H_9		84.4 ± 0.9	25.9 ± 1.7	46.5 ± 1.5	38.0 ± 1.0	43.8 ± 0.4
14	CH_3	C_5H_9	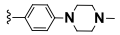	58.0 ± 1.0	52.2 ± 0.7	65.4 ± 1.3	42.7 ± 0.6	63.1 ± 0.5
15	C_5H_9	CH_3	2-OHPh	34.9 ± 1.0	27.1 ± 1.1	66.1 ± 1.7	40.6 ± 0.6	56.8 ± 0.6
16	C_5H_9	CH_3	3-CF_3Ph	32.6 ± 1.0	25.8 ± 0.9	44.8 ± 1.5	37.0 ± 0.6	61.6 ± 1.2

17	C_5H_9	CH_3	4-$N(CH_3)_2$Ph	81.6 ± 1.3	60.2 ± 1.6	81.0 ± 0.9	51.9 ± 0.6	72.8 ± 0.6
18	C_5H_9	CH_3	Ph	80.7 ± 0.8	26.4 ± 0.5	46.3 ± 1.9	37.4 ± 0.5	45.5 ± 0.5
19	C_5H_9	CH_3	4-CF_3Ph	70.0 ± 1.5	27.8 ± 0.9	56.3 ± 1.0	36.0 ± 0.4	50.2 ± 1.1
20	C_5H_9	CH_3	4-NH_2Ph	53.6 ± 2.0	54.4 ± 0.6	73.6 ± 1.3	56.1 ± 0.7	73.2 ± 1.0
21	C_5H_9	CH_3	2-NH_2Ph	66.3 ± 1.3	27.5 ± 0.7	44.1 ± 1.1	36.5 ± 0.4	63.4 ± 0.7
22	C_5H_9	CH_3	2-NH_2,4-FPh	64.6 ± 1.9	26.8 ± 0.7	67.2 ± 0.8	36.8 ± 0.5	74.0 ± 0.4
23	C_5H_9	CH_3		21.7 ± 2.3	29.3 ± 1.2	61.6 ± 0.7	36.7 ± 0.4	50.9 ± 1.0
24	C_5H_9	CH_3	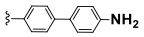	39.2 ± 1.1	30.5 ± 1.3	51.8 ± 0.9	36.1 ± 0.4	46.4 ± 0.3
25	C_5H_9	CH_3		67.9 ± 2.0	29.5 ± 0.8	42.0 ± 0.8	39.9 ± 0.6	44.7 ± 0.6
26	C_5H_9	CH_3	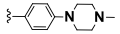	59.0 ± 1.7	43.3 ± 0.6	69.7 ± 1.0	40.4 ± 1.0	52.4 ± 0.7
		Rolipram		87.1 ± 1.2	39.8 ± 1.8	85.4 ± 1.8	54.6 ± 1.1	78.4 ± 0.9

Note: The table showed that the cytotoxicity of the compounds at 100 μM and neuroprotective effects against glutamate- and acrolein-induced neuronal injury at 3 and 10 μM in HT22 cells. The cell viability was expressed as the percentage of control group. The data were expressed as the mean ± SD, $n = 6$.

Table 2-1. Physicochemical properties of compound 5

Compd.	LogP	M.W.	Rotatable bonds	H-bond acceptors	H-bond donors	Caco2 permeability (Pe)	CNS penetration (Score)
5	4.26	380.48	8	3	1	230E-6	-2.69

Note: M.W.: molecular weight; **LogP:** logarithm of the octanol-water partition coefficient;

Table 2-2. ADMET prediction of compound 5

Compd.	GI absorption	BBB permeant	Pgp substrate	CYP1A2 inhibitor	CYP2C19 inhibitor	CYP2C9 inhibitor	CYP2D6 inhibitor	LD_{50} ≤ (mg/Kg)	LD_{50} ≥ (mg/Kg)
5	High	Yes	No	No	Yes	Yes	Yes	5000	300